

12 LEVEL III  
85

AD

AD-E460 566

TECHNICAL REPORT ARLCD-TR-80037

TORSIONAL IMPULSE IN GUN LAUNCHED PROJECTILES

ALBERTUS E. SCHMIDLIN

AD A 096799

MARCH 1981

DTIC ELECTE  
MAR 24 1981  
S B D



US ARMY ARMAMENT RESEARCH AND DEVELOPMENT COMMAND  
LARGE CALIBER  
WEAPON SYSTEMS LABORATORY  
DOVER, NEW JERSEY

APPROVED FOR PUBLIC RELEASE: DISTRIBUTION UNLIMITED.

DTIC FILE COPY

81 3 11 003

The views, opinions, and/or findings contained in this report are those of the author and should not be construed as an official Department of the Army position, policy or decision, unless so designated by other documentation

Destroy this report when no longer needed Do not return to the originator

The citation in this report of the names of commercial firms or commercially available products or services does not constitute official endorsement or approval of such commercial firms, products, or services by the US Government

UNCLASSIFIED

SECURITY CLASSIFICATION OF THIS PAGE (When Data Entered)

REPORT DOCUMENTATION PAGE		READ INSTRUCTIONS BEFORE COMPLETING FORM
1. REPORT NUMBER Technical Report ARLCD-TR-80037	2. GOVT ACCESSION NO. AD-A096	3. RECIPIENT'S CATALOG NUMBER 799
4. TITLE (and Subtitle) TORSIONAL IMPULSE IN GUN LAUNCHED PROJECTILES	5. TYPE OF REPORT & PERIOD COVERED Final 1977-1980	
7. AUTHOR(s) Albertus E. Schmidlin	8. CONTRACT OR GRANT NUMBER(s)	
9. PERFORMING ORGANIZATION NAME AND ADDRESS ARRADCOM, LCWSL Nuclear and Fuze Div (DRDAR-LCN- ) Dover, NJ 07801	10. PROGRAM ELEMENT, PROJECT, TASK AREA & WORK UNIT NUMBERS	
11. CONTROLLING OFFICE NAME AND ADDRESS ARRADCOM, *SD STINFO Div (DRDAR-TSS) Dover, NJ 07801	12. REPORT DATE March 1981	13. NUMBER OF PAGES 62
14. MONITORING AGENCY NAME & ADDRESS (if different from Controlling Office)	15. SECURITY CLASS (of this report) Unclassified	
16. DISTRIBUTION STATEMENT (of this Report) Approved for public release; distribution unlimited.		
17. DISTRIBUTION STATEMENT (of the abstract entered in Block 20, if different from Report)		
18. SUPPLEMENTARY NOTES		
19. KEY WORDS (Continue on reverse side if necessary and identify by block number) Projectiles                      Computer modeling Joints                              XM550 projectile Threaded assemblies          XM549 projectile Torsional impulse              Angular acceleration Stress		
20. ABSTRACT (Continue on reverse side if necessary and identify by block number) This report describes an investigation of torsional impulse in rocket-assisted projectile, due to "free run." A combined analytical and experimental program was carried out to quantify the phenomenon. The basic factor was the presence of "free run" which is characterized by positive forward motion of a projectile before reaching the origin of gun-tube rifling. This factor permits the projectile to reach an appreciable forward velocity before the rotating band becomes effective and starts the rotational acceleration. (cont. invad)		

DD FORM 103

REVISION OF 1 NOV 68 IS OBSOLETE

UNCLASSIFIED

SECURITY CLASSIFICATION OF THIS PAGE (When Data Entered)

UNCLASSIFIED

SECURITY CLASSIFICATION OF THIS PAGE (When Data Entered)

Experiments were also conducted by Sandia Laboratories-Livermore with instrumentation installed in the rocket motor section.

The results indicate that the amplitude of the angular acceleration pulse due to free run was greater in tubes with more wear. The acceleration pulse was higher at the nose than at the rear of the projectile and the magnitude of the acceleration pulse in worn tubes was as great as and in some cases (8 inch) greater than the predicted angular acceleration at peak pressure.

Test results at ARRADCON and Sandia were in qualitative agreement. The point where the angular acceleration pulse occurs seems to correlate with the position of travel where a sufficient amount of rotating band material has been formed (swaged) in the gun tube rifling.

UNCLASSIFIED

SECURITY CLASSIFICATION OF THIS PAGE (When Data Entered)



## CONTENTS

	Page
Introduction	1
Computer Simulation	2
Threaded Joint	3
Experimental Programs	4
Test Series	4
Effect of Gun Tube Wear	10
Conclusion:	15
Recommendations	16
References	17
Distribution List	19

## TABLES

	Page
1. Torsional impulse testing of 8-inch M110E1 cannon with cut-back band	7
2. Torsional impulse testing of 155-mm, M198 howitzer, proof (PxR 6255) charge	11
3. Torsional impulse tests -- comparison of ARRADCOM and SLL tests in tube no. 83	14

## FIGURES

	Page
1 Special test firing - 8-inch projectile	19
2 Computer model - XM753	19
3 8-Inch joint - thread and knurled face	20
4 Torque at joint - 1 inch free run	20
5 Coefficient of friction for no tightening	21
6 Shear stress at thread - coefficient of 0.1	21
7 Maximum thread stress - coefficient of 0.1	22
8 Experimental and computer results - 1 inch free run	22
9 Torsional impulse test round - XM650	23
10 8-Inch rotating band - old and new	23
11 Tangential acceleration versus distance - old band	24
12 Tangential acceleration versus distance - new band	25
13 Averaged test results	26
14 Torsional impulse test round - 8-inch	27
15 Ratio tangential to axial accelerations at collector cup - 8-inch	28
16. Tangential acceleration versus time collector cup - 8-inch	29
17 Tangential acceleration versus travel - collector cup - 8-inch	30
18 Axial acceleration versus time - 8-inch	31
19 Tangential versus axial velocities - 8-inch	32
20 Torsional impulse test round - 155-mm	33

21	Ratio of tangential to axial accelerations versus travel at motor body - worn tube - 155-mm	34
22	Ratio of tangential to axial accelerations versus time at motor body - worn tube - 155-mm	35
23	Tangential accelerometer #2127 at motor body versus time - 155-mm	36
24	Tangential accelerometer #2130 at motor body versus time - 155-mm	37
25	Axial accelerometer versus time - 155-mm	38
26	Tangential accelerometer #979 at collector cup versus time - 155-mm	39
27	Difference in tangential accelerometers versus time round #2321 in worn tube - 155-mm	40
28	Difference in tangential accelerometers versus time round #2320 in worn tube - 155-mm	41
29	Tangential versus axial velocities - 155-mm	42
30	Gun tube profiles - 8-inch XM203	43
31	Gun tube profiles - 155-mm XM39	43
32	Silhouettes of rotating bands - 155-mm and 8-inch projectiles	40
33	Overlap of band in rifling profiles - 8-inch	45
34	Overlap of band in rifling profiles - 155-mm	46
35	Band/rifling overlap in ARRADCON and Sandia tests	47

## INTRODUCTION

During the development testing of an 8-inch rocket-assisted projectile in December 1976, a malfunction occurred which caused the first few rounds of the scheduled firings to fall short of predicted range. Examination of the recovered projectile showed that a structural failure had occurred and that the rocket motor had rotated in a clockwise (tightening) direction. This motor body rotation sheared the threads of the joint at the bulkhead and severed the telemetry (TM) cable, causing a loose joint and TM signal failure. The loose joint affected the normal projectile flight profile such that the range attained was 5 km short of the requirement. Further inspection of the hardware showed the motor bulkhead joint surfaces to be contaminated with a greasy substance (thread sealant and silicone compound) (ref 1).

Firing records showed that after final raising and seating into the forcing cone of the gun tube, the projectile still had an axial travel (free run) of approximately 25 mm (1 in.) before the rotating band engaged the origin of rifling. It was concluded that axial acceleration of the projectile, interrupted momentarily by sudden rotating band/tube rifling engagement, caused a torsional impulse which was transmitted through the bulkhead joint and thereby created an abnormally high torsional load on the threaded joint. This high load at a time of relatively low axial setback force on the face of the joint, overtaxed the available coefficient of friction, allowed relative motion and the eventual failure of the thread. A special test projectile was prepared to duplicate these conditions. The results of the firing are shown in figure 1.

As a result of this malfunction and in view of the possibility of a potentially greater free run because of dimensional tolerances, wear in the gun tube, etc., an exhaustive investigation of torsional impulse in gun launched projectiles was undertaken. These efforts entailed analytical modeling and experimental verification and were conducted by both the Large Caliber Weapon Systems Laboratory (ARRADCOM) and the Sandia Laboratories Livermore (SLL).

The purpose of these investigations was to characterize the in-bore environment when the projectile was subjected to free run in the gun tube. The effect of this condition was particularly important in nuclear projectiles since they involve more complex warheads which may be adversely affected by these unwanted dynamic load conditions. Both 8-inch and 155-mm projectiles were analyzed. The investigation included analytical modeling which used the Super Sceptre computer program and experimental testing which used modified XM550 and XM569 projectiles, respectively.

The experiments were conducted with the use of a wire-in-bore technique. This procedure provides hard wire communication between the instruments on board the projectile and the recorder in the ground station. This report is concerned primarily with the analysis of the experimental data and it documents procedures to derive the maximum amount of information from the tests. Testing of this type is necessarily difficult since the instrumentation is subjected to the high setback forces along the axis of the projectile and the extreme lateral forces due to balloting, etc., while at the same time sensing the angular motion about the projectile axis. Therefore, the recorded signals might well contain much extraneous information.

Sandia Laboratories used a telemetry package for data transmission rather than the wire-in-bore technique used at ARRADCOM. The results of Sandia's investigation complement the work reported at ARRADCOM and present a useful cross-check of the nature and magnitude of the torsional impulse phenomenon. Quantitative results from the two investigations are in reasonable agreement.

#### COMPUTER SIMULATION

After the failure of the 8-inch projectile, efforts were started to quantify the magnitude of the loads due to a free run condition. A computer simulation of the 8-inch XM753 projectile was made with the use of the Super Sceptre technique (ref 2). Super Sceptre is a program for the analysis of electrical, mechanical, digital and control systems (ref 3), for application of this technique, the dynamic system is broken up into a group of equivalent masses, springs, forcing elements, etc. The 8-inch projectile was divided into several sections (fig. 2).

The rocket motor is described by a moment of inertia,  $I_1$ , a spring constant,  $K_1$ , a rotational velocity,  $\omega_0$ , corresponding to the twist of the rifling, and a rotational velocity,  $\omega_1$ , corresponding to the actual rotating band speed. The warhead is described by three moments of inertia,  $I_4$ ,  $I_6$  and  $I_5$ , interconnected by resilient members having spring constants  $K_3$  and  $K_2$  respectively. The coupling of the spring,  $K_1$ , to the inertial element,  $I_6$ , is at the joint which is the subject of this investigation. This model is also used for the projectile used in the test program, the XM659. In this case  $I_6$  and  $K_3$  are eliminated and the equivalent moment of inertia is included in  $I_4$  and  $I_5$ .

The computer program simulates the dynamic conditions which occur in the gun tube. The projectile is acted upon by the base pressure,  $P_0$  (fig. 2) which is the effective pressure on the base which is available for acceleration. (This is in agreement with

the definition given in reference 4). The Super Sceptre program calculates axial acceleration, velocity, and displacement as a function of time. The rotational energy in the projectile is assumed negligible with respect to the translational energy and therefore is not calculated. This difference is about 1%.

As the projectile moves forward, it encounters the rifling at the end of the free run. At this time, the rotation of the projectile starts and the computer begins to consider it as a rotating body. In this analysis the rotational dynamics are coordinated with translation but the computations are done separately, as if on a separate body. The computer simulation is described in more detail in reference 2.

### THREADED JOINT

A mathematical model of the 8-inch threaded motor joint comprised of both the knurled annular end faces and the weakest of the two threads; i.e., the male bulkhead thread, is included in the computer program. The buttress thread is modeled as a jackscrew; frictional effects are included at the thread as well as at the knurled faces. The model calculates the bearing stress at the faces of the knurls and of the thread, the average and maximum shear stresses at the root of the thread, and the bending stress at the root of the thread. The coefficient of friction can be varied as one of the parameters. In addition, the friction required for no slip at the knurled faces is computed. The percentage of effective threads and effective bearing areas at the faces of the knurl can also be varied.

A sketch of the thread is shown in figure 3. The force transmitted at the knurled face is  $F_1$ , and the shearing force on the thread is  $F_2$ . The force due to base chamber pressure is transmitted through the rocket motor body and is designated by  $F_3$ . Before firing,  $F_3$  is zero and  $F_1 = F_2$ . At this point the forces are the result of the initial torque at assembly. During firing  $F_3 = M_{wh} \ddot{X}$  where  $M_{wh}$  is the mass of the warhead; that is, everything forward of the joint. The force equation then is  $F_3 = F_1 - F_2$ . This expression and the formula for a jackscrew are used to calculate the stresses at several critical areas in the joint. A detailed description of the threaded joint is given in reference 2. Typical results of the computer simulation are given in figures 4 through 8.

The torsional impulse which occurs at the joint with a free run of 25.4 mm (1 in.) is shown in figure 4. It is apparent that the peak value is greater than the usual maximum which occurs at peak chamber pressure. Its effect is accentuated because it occurs

when the setback force and therefore the torque transmitted by friction at the knurled face, are small. Figure 5 shows the instantaneous coefficient of friction which is necessary to prevent tightening of the joint under these conditions. The peak value is 0.3 which might not be satisfied if the knurl is imperfect and/or the joint is contaminated with a foreign material which may act as a lubricant.

For an assumed coefficient of friction of 0.1, figure 6 illustrates slippage at the knurled faces which allows the joint to tighten thereby increasing the stress in the threads. The free run is 25.4 mm (1 in.) and the effective engagement of the thread is assumed to be 100%. For a thread which is less than perfect, there is a potential failure problem. Figure 7 shows this result for a coefficient of friction of 0.1 and large and small free runs, respectively. It is apparent that a thread which is 80% perfect is marginal with large free run but safe with small free run. The margin of safety with imperfect threads is considerably increased when free run is not present.

Finally, the computer results were compared with the averaged experimental results for a free run of 25.4 mm (1 in.) (fig. 8). Tangential acceleration at the installed radius of the sensors are plotted versus the distance traveled by the projectile. The results correlate well as far as peak amplitude is concerned but differ in the width of the pulse.

#### EXPERIMENTAL PROGRAMS

##### Test Series

##### 8-Inch Projectiles

Two series of tests were conducted in a modified XM650 projectile to quantify the torsional impulse in the 8-inch family of projectiles. In the first set, one axial and two tangential accelerometers were mounted in a special fixture at the front of the projectile (fig. 9). This fixture matched the weight of the forward material it replaced. Ten rounds were fired in this manner at Yuma Proving Ground.

The propelling charge was the M188E1, zone 9, conditioned at 63 C (145 F). The XM201 tubes were used, tube no. 14 with a 63% remaining life and tube no. 27 with a 5% remaining life. Two rotating bands were evaluated in each tube. The first was the standard band at that time (January 1977) on the conventional 8-inch RAP round and the second was a cut-down version which permitted band seating within 2.3 mm (0.09 in.) of the origin of rifling. A com-

parison of the rotating band details is pictured in figure 10. Typical results with the standard band and the cut band are shown in figures 11 and 12, respectively.

Analyzing the test results was difficult because of severe high frequency oscillations. It was not evident at this point whether or not these frequencies were true indications of the dynamic motion of the projectile. It was evident, however, that there was a higher peak in initial acceleration of the projectiles with the band which permitted more free run. Test results after smoothing and averaging are shown in figure 13. Here the results are shown in nondimensional form by plotting the ratio of the tangential to axial accelerations versus distance travelled.

In the second set of tests, accelerometers were installed both at the front of the projectile and at the rear (fig. 14). Again the weight was distributed to match the mass properties of the conventional round. Eleven projectiles were fired at Yuma Proving Grounds in three different tubes in August 1978.

The propelling charge was the M188E1, zone 9, conditioned at 57 C (135 F). Three XM201E1 tubes were used to provide tests under new, used and worn out conditions. Tube no. 28 after 600 rounds represented the new tube; tube no. 8268 after 880 rounds, the used or mid-life tube; and tube no. 23 after 1460 rounds, the worn tube. In these tests all rotating bands were of the new, cut-back design which theoretically permits only 23 mm (0.09 in.) of travel in a new tube before engagement with the rifling.

Analysis of these tests revealed that:

1. The amplitude of the angular acceleration pulse was greater in tubes with more wear.
2. The acceleration pulse was higher at the front than at the rear of the projectile.
3. The magnitude of the acceleration pulse in worn tubes was greater than the predicted angular acceleration at peak pressure.

An example of the results of this testing is shown in figure 15. Here the ratio of the peripheral to axial accelerations is plotted versus axial travel of the projectile. As travel increases, the graph approaches the theoretical value of  $\pi/20$  or 0.157 for full engraving. If all instruments were perfect and

there were no other errors, the graphs would approach the theoretical value. The axial travel is used as the abscissa because of the significance in this investigation of axial motion relative to engagement by the rotating band in the rifling. A comparison of graphs plotted against time and travel is shown in figures 16 and 17. A plot of axial acceleration is shown in figure 18.

Tangential acceleration at the skin of the projectile plotted as a function of time, is shown in figure 16. It indicates that relatively little acceleration is present for half of the total time and this is followed by large oscillatory signals. Figure 17 shows the same variable plotted against the distance travelled by the projectile. The major oscillatory signals are present over most of the graph and only small oscillations occur over the first 40 mm (1.6 in.) of travel. Actually it seems evident that some of the initial oscillations are due to lateral motion during the time that the rotating band is undergoing the initial swaging or engraving process and before any appreciable rotational motion occurs. It is important to discern the beginning of rotational motion as a function of the distance travelled (fig 17).

Another advantage of the graphs that are plotted versus distance travelled is that they allow comparison of different projectiles independent of the synchronization of the time base. Variations in the starting time of data reduction are cancelled out when graphs are plotted versus the distance travelled.

The axial acceleration versus time is shown in figure 18. The oscillations which begin at 5 milliseconds occur as the torsional impulse develops (fig 16).

The effect of free run and the torsional impulse which is associated with the start of the rotational motion of the projectile, can be pictured by comparing simultaneous values of tangential and axial velocities. A plot of these two variables is shown in figure 19. It is obvious from the graph that the projectile is delayed in starting its rotation while at the same time it is building up axial velocity, reaching more than 30 meters per second (100 feet per second) before rotation begins. When the rotating band finally takes hold, the tangential acceleration is very high, causing the velocity to overshoot the theoretical value. Finally, the ratio of the two velocities reaches the theoretical figure just before the end of useful signal transmission.

Test results of the 8-inch test projectile are summarized in table 1.

Table 1. Torsional impulse testing of 8-inch M10E1 cannon  
with cut-back band

<u>Gun Tubes Tested</u>						
<u>Gun tubes</u>	<u>SN</u>	<u>Land wear</u> (diameter)		<u>Groove wear</u>		<u>No. of rounds</u>
		<u>mm</u>	<u>(in.)</u>	<u>mm</u>	<u>(in.)</u>	
New	XM201 28					600
Mid-life	M201 8268	1.52	(0.060)	0.15	(0.006)	882
Worn	XM201 23	2.56	(0.101)	1.42	(0.056)	1462

<u>Test Result</u>			
<u>Conditions</u>	<u>New</u>	<u>Mid-life</u>	<u>Worn</u>
Acceleration pulse, rad/sec <sup>2</sup>			
at motor	70,000	100,000	165,000
at collector	100,000	145,000	215,000
Travel at pulse, mm (in.)	35.6 (1.4)	53.3 (2.1)	81.3 (3.2)
Setback at pulse, g's	2200	3000	4200

Note: All tests were conducted with zone 9

## 155-mm Projectiles

A series of tests were conducted in a modified M549 projectile to quantify the torsional impulse in the 155-mm family of projectiles. Accelerometers were installed both at the front and rear as shown in figure 20. Again, the weight was distributed to match the conventional round. In this case a completely new forward body was designed to accommodate the forward accelerometers in the collector cup rather than to rework the conventional warhead section as was done in the 8-inch. Twelve projectiles were fired at Yuma Proving Grounds in August 1978.

The propelling charge was the proof (PXR 6255) charge. Three XM199 tubes were used to provide tests under new, used and worn conditions. Tube no. 27682 represented the new tube; no. 75 after 1065 rounds, the used or mid life tube; and no. 83 after 2322 rounds, the worn tube. The worn tube was chrome-plated while the other two were steel tubes. In all tests the rotating bands were of the standard M549 design. Contrary to the situation in the 8-inch system, after ramming, the rotating band of the M549 overlaps the origin of rifling in the forcing cone. Therefore, theoretically in a new tube there is no free run in the usual sense. Actually there is an effective free run, albeit small, because the rotating band must undergo a finite amount of engraving before rotation can start. This fact is indicated by the test results.

Analysis of these tests indicated several significant results, some of which are the same as the 8-inch case:

1. The amplitude of the angular acceleration pulse was greater in tubes with more wear.
2. The acceleration pulse was higher at the front than at the rear of the projectile.
3. The magnitude of the pulse in a worn tube was approximately the same as the predicted angular acceleration at peak pressure, not higher as in the case of the 8-inch projectile.

It was also evident that the 155-mm results showed appreciably more noise and inconsistency in the signals. In some cases an analytical technique was used to compensate for these effects and obtain meaningful information from otherwise inconsistent data.

A scheme for correcting the inconsistency due to the effect of cross axis sensitivity of the accelerometers was particularly useful.

An example of the results of this testing is shown in figure 21. This case represents the most severe result in this series. It should be emphasized here that the gun tube in this test was a badly worn chrome-plated tube. This condition is one of the most severe and is discussed in depth in this report. The peak ratio in figure 21 is 0.54 compared to 0.157 for perfect engraving. Therefore, there is an amplification factor of  $0.54 \div 0.157 = 3.40$  which means that the angular acceleration (and the corresponding torque in any joint in the projectile) is 3.4 times the expected value under normal acceleration of the body. This also means that the required coefficient of friction in a threaded joint must be 3.4 times the normal expected value. Hence, it is apparent that threaded joints, especially those positioned aft of the warhead section, are a potential problem when severe torsional impulse is present.

The graph in figure 22 shows the same plot with time as the independent variable. It is evident once more that the oscillations seen initially are not significant in this investigation since they occur before the projectile has moved an appreciable distance (5 mm (0.2 in.)) well before the torsional peak which occurs at 40 mm (1.56 in.).

Figures 21 and 22 are based on the average of the two tangential accelerometers in the motor body. Graphs of the individual accelerometers are given in figures 23 through 26 plotted against time. Tangential accelerometers at the motor body are shown in figures 23 and 24. The axial accelerometer is pictured in figure 25. One of the tangential accelerometers in the collector cup is shown in figure 26. The other tangential accelerometer channel failed in this test. The amplification of the torsional impulse at the front of the body is evident by comparing figure 26 with the motor body sensors.

Another significant factor is that as the projectile moves into the rifling, the ratio of the average tangential acceleration to the axial acceleration approaches the theoretical asymptote at 0.157 (fig. 21). This tends to confirm the validity of the test data because, theoretically, a fully engraved rotating band should produce this result. Furthermore, inspection of figures 23 and 24 shows that each graph is of the same nominal magnitude and hence the average is a true average, not distorted by the combination of individual higher-than-normal and lower-than-normal signals. Another test for the consistency of these data can be made by calculating and plotting the average difference in the two signals. This calculation gives the net lateral acceleration of the projectile. A sustained signal level for a long period of time is not feasible since this would imply excessive lateral motion. The

lateral travel is limited by the clearance between the projectile and the gun tube. Examination of figure 27 shows a graph which is predominantly oscillatory at about 2.5 kHz. This feature is acceptable and indicates a lateral oscillation or vibration in the tube.

An example of an undesirable curve is one which has a decided trend in the positive direction to such an extent that a fallacy in the data must be assumed (fig. 28). Results of this type cast doubts on three out of four tests in some cases. Analysis of the effect of cross-axis sensitivity on these experiments resulted in development of a factor which corrected two out of the three cases. This factor, which is based on a linear model of the errors, was used in compiling the averaged results of the tests.

The effect of free run and the associated start of the rotational motion can be pictured by comparison of simultaneous values of tangential and axial velocities as was done earlier for the 8-inch projectile. A plot of these two variables is shown in figure 29. It is obvious that the projectile is delayed in starting its rotation while at the same time it is building up axial velocity, reaching more than 30 meters per second (100 feet per second) before rotation begins. When the rotating band finally takes hold, the angular acceleration is very high, causing the velocity to rise sharply and approach the theoretical steady state value. In the graph shown, a 2% cross-axis sensitivity would account for the difference between the curve and the theoretical asymptote, a reasonable figure to expect in these tests.

The results of the 155-mm projectile tests are summarized in Table 2.

#### Effect of Gun Tube Wear

The tabulated results for both the 8-inch and 155-mm projectiles (tables 1 and 2) show that the torsional impulse increases with wear in the tube. To portray the geometrical picture, a series of layouts were made of the rifling in the gun tube as related to the profile of the rotating band at various positions of travel. The profiles of the gun tube were drawn with use of the star-gage measurements. An exaggerated scale for the wear patterns was used for plotting these profiles. Examples of these plots for the 8-inch XM201 tubes and the 155-mm XM199 tubes are shown in figures 30 and 31. The silhouettes of the rotating band and obturator were also drawn to the same scale (fig. 32).

Table 2. Torsional impulse testing of 155-mm, M198 howitzer, proof (PXR) 6255 charge

<u>Gun tubes</u>		<u>SN</u>	<u>Gun Tubes Tested</u>				<u>No. of rounds</u>
			<u>Land wear (diameter)</u> <u>mm (in.)</u>		<u>Groove wear</u> <u>mm (in.)</u>		
New	M199	27682					6
Mid-life	XM199E	75	1.40	0.055	0.25	0.010	1065
Worn	XM199	83	1.78	0.070	0.05	0.002	2322

Results averaged

<u>Conditions</u>	<u>New</u>	<u>Mid-life</u>	<u>Worn</u>
Acceleration pulse, rad/sec <sup>2</sup>			
at motor body	Small*	100,000 <sup>+</sup>	260,000
at collector cup	Small*	130,000	290,000 <sup>+</sup>
Travel at pulse, mm (in.)	7.6 (0.3)	30.5 (1.2)	38.0 (1.5)
Setback at pulse, g's	2,000	3,000	4,200
Peak breech press, MPa (kpsi)	412 (59.8)	419 (60.8)	431 (62.5)

\* An impulse is indicated but results preclude quantification

+ Result of a single measurement

With the aid of transparencies, the silhouette of the band area can be superimposed on the layout of the gun tube rifling to illustrate the degree of engraving as a function of the travel of the projectile. The overlap of the rotating band profile into the grooves of the rifling is an indication of the amount of band material which has been swaged or engraved as the projectile accelerates. Although consideration is not given to actual deflections such as the elastic deformations which occur under actual gun load conditions, it seems accurate enough to develop a qualitative correlation between the engraving process and the torsional peak which occurs in a gun tube with free run. Several cases illustrating this technique are shown in figures 33 and 34.

The tests of the 8-inch projectile are summarized in table 1. Listed in the table is the travel at the point where the acceleration pulse occurs in each tube. With this information and the wear profiles of the tubes, the overlap of the rotating band can be shown when the torsional pulse occurs in each case (fig. 33). It is apparent that the overlap, or engagement, of the band in the rifling is least for tube no. 28 which has the least wear. This case also requires the smallest torsional pulse to start the projectile in motion, a fact that is compatible with the small overlap. In tube no. 8268 (in the intermediate wear condition), the overlap or engraving is greater and so is the torsional pulse. Here again, the degree of overlap is compatible with the torque requirement. Finally, the overlap in tube no. 23 shows the greatest of all three cases. The torsional peak is greatest and again the consistency, although qualitative, is confirmed (table 1).

The tests of the 155-mm projectile are summarized in table 2. The magnitude of the average travel condition in each case is specified. Overlap layouts were made as before (fig. 34). Here it is especially apparent that in the new tube the free run is small and the torsional pulse for all intents and purposes is not present. Table 2 shows a small pulse at a travel of 7.6 mm (0.3 in.) It is apparent from the figure that the overlap is minimal for this case. In tube no. 75, the mid-life tube, the torsional pulse is greater and so is the overlap. Hence, the overlap layout confirms the geometric engagement which is necessary to produce the torque for acceleration of the projectile. Finally in the tube no. 83, a badly worn specimen, the greatest overlap is illustrated. This case also exhibits the greatest torsional pulse and the consistency of band overlap versus torque requirement is maintained. It should be pointed out that the proof charge (PXR 6255) provides an over-test condition as illustrated by the high breech pressures recorded in table 2.

Comparison of results from tests made on tube no. 83 by ARRADCOM in August 1978 and tests made by Sandia Laboratories-Livermore in March 1979 indicated that Sandia experienced greater torsional peaks due to free run (table 3, reference 5). Of particular significance is the additional number of rounds fired and the associated wear of the tube between the time of the ARRADCOM tests and the Sandia tests. Overlap layouts were made to illustrate the geometric relationships for the two cases. Evidently the additional wear at the rifling in the Sandia tests did not extend rearward into the forcing cone because both ARRADCOM test round 2319 and Sandia test round FG 129 were rammed to the same depth (40 1/2 in.). The travel reached by each projectile at the point where the torsional impulse occurred was different, however. Furthermore, the peak pulse was 25% greater in the Sandia test. Both of these factors are compatible with the stargage wear measurements of the tube.

The overlap layouts in figure 35 again provide an interesting insight into the geometric engagement of the rotating band in the rifling. As shown in the figure, the results confirm the fact that the magnitude of the acceleration pulse requires a comparable overlap area that is, a comparable amount of engraving or swaging before the torque-producing capability is reached at the rotating band. When this condition is met, the torque builds up suddenly and the projectile is given a very large angular acceleration. Finally, as the band enters into its fully engaged position, the projectile is brought up to its normal rotational speed which is proportional to linear speed.

Significant positions of travel for each projectile are illustrated in figure 35. Positions after ramming are shown as well as the wear profiles of tube no. 83 after 2322 rounds (ARRADCOM) and 2670 rounds (Sandia). Also depicted is the overlap position when the torsional pulse occurred in ARRADCOM round no 2319 which had traveled 39-mm (1.5 in.) and attained a velocity of 46 m/sec (150 ft/sec). Shown here in cross section is the amount of band material which has been engraved. Round no. FG 129 in the SLL test is shown at the same position of travel. The amount of band material is much less in this case and this condition implies that severe scarring and slippage of the band are occurring at this point. The SLL band does not take hold until additional travel occurs. After the band moves 51-mm (2.0 in.), its torsional strength is sufficient to supply the demand and a sizable torsional pulse occurs. Table 3 shows that this added motion in the SLL tests was accompanied by an increase in velocity to 59 m/sec (195 ft/sec) before the rotating band took hold, thereby creating a more severe impulsive condition. This condition resulted in a torsional impulse having 1.25 times the peak magnitude of the ARRADCOM test round.

Table 3. Torsional impulse testing — comparison of ARRADCOM and SLL tests in tube No. 81

	<u>ARRADCOM</u>	<u>SLL</u>
Test round no.	2319 2320 2321 2322	PG 129 PG 131
Test conditions		
No. rounds at stavage	2322	2670
Average torsional pulse, rad/sec <sup>2</sup>	260,000	320,000
Travel at pulse, mm (in.)	38.0 (1.50)	53.3 (2.1)
Average axial velocity at pulse, m/sec (ft/sec)	46 (150)	59 (195)
Average maximum axial acceleration g's	16,000	12,200

\*Calculated from filtered data.

The wear pattern in tube no. 83 illustrates a tube condition which is no longer acceptable for tactical use because of the high torsional impulse and also the fact that the band was stripped away in the SLL tests.

### CONCLUSIONS

As a result of the analytical study, it is evident that in an 8-inch projectile a threaded joint which transmits the torque necessary to accelerate a heavy warhead can be marginal when a combination of factors is present. These factors are a worn tube and/or a rotating band design which allows free run, an unsatisfactory finish on the mating parts and the presence of a fluid contaminant which can degrade the coefficient of friction.

The experimental study confirmed the order-of-magnitude of the peak torque predicted by the computer analysis for a free run of 25-mm (1 in.). For a small free run which is estimated as 2.3-mm (0.09 in.) based on the drawings, the computer analysis underestimates the peak torque by about 50%. When the actual free run is used as computer input, the peak torque prediction is within +20%.

The experimental results indicated several significant factors:

1. The amplitude of the angular acceleration pulse due to free run was greater in tubes with more wear.
2. The acceleration pulse was higher at the nose than at the rear of the projectile.
3. The magnitude of the acceleration pulse in worn tubes was as great as and in some cases (8-inch XM650) greater than the predicted angular acceleration at peak pressure.

Worn chrome-plated tubes seemed to introduce a more severe torsional impulse due to free run than steel tubes having the same maximum wear dimensions. This is due to the wear distribution in chrome tubes which occurs during the first few inches of rifling and suddenly falls off to no wear at all.

The point at which the peak torque occurs seems to correlate with the position during travel where the amount of rotating band material which was engraved is commensurate with the torque which is needed to bring the projectile "on the line" in rotation.

## RECOMMENDATIONS

It is recommended that a study be made and a compilation prepared of the wear profiles and dimensions of gun tubes used (or which may be used) in experimental tests of the type described in this report. This information could be correlated with the torsional impulse test data. Through this procedure, a data bank of cause-and-effect information could be assembled and a rational basis developed to predict torsional impulse levels as a function of the condition of the worn gun tube.

## REFERENCES

1. D. J. Savory, "Failure Analysis and Evaluation -- Rocket Motor Warhead Joint Design, Projectile, 8-Inch, RAP, Nuclear: XM753," Interim Technical Report NAD 101, LCWSL, USARRADCOM, June 1977.
2. A. E. Schmidlin, "Computer Simulation of Projectile Motion in a Gun Tube with Free Run, Fourth International Symposium on Ballistics, ADPA, Monterey, California, October 1978.
3. J. C. Bowers et al, Users Manual for Super Sceptre, AD-A011348, University of South Florida, Tampa, Florida, May 1975.
4. L.D. Heppner, "Setback and Spin for Artillery, Mortar, Rifle and Tank Ammunition, Technical Report APG-MT-4503 Aberdeen Proving Ground, Maryland, September 1974.
5. J. E. Didlake, "Results of Balloting and Torsional Impulse," presented to the XM785 Environmental Working Group, 12 & 13 Sept 1979, "Sandia Laboratories-Livermore, California, March 1980.



Figure 1. Special test firing - 8-inch

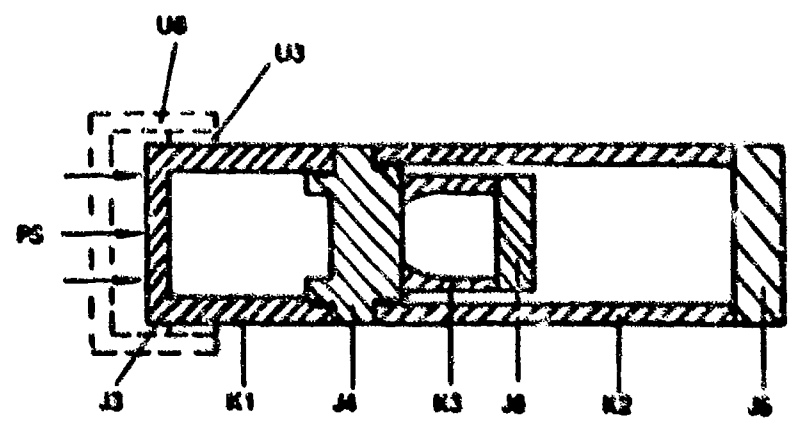


Figure 2. Computer Model - XN753

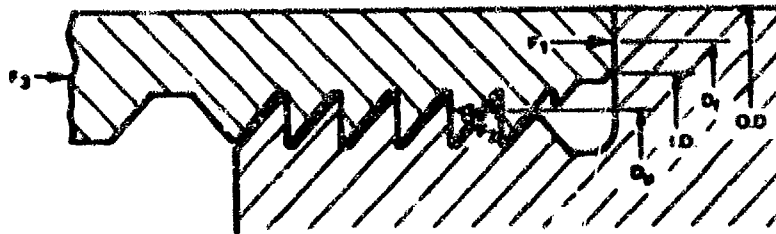


Figure 3. 8-inch Joint - thread and knurled face

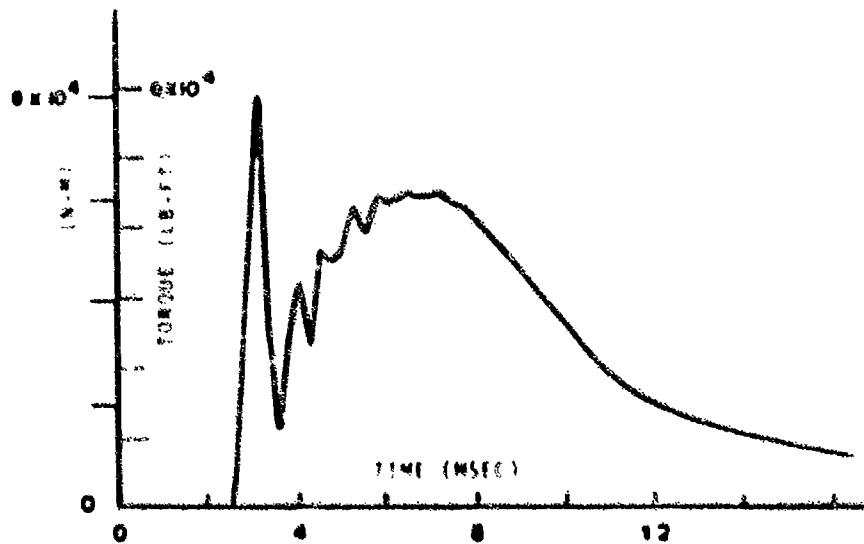


Figure 4. Torque at joint - 1 inch free fun

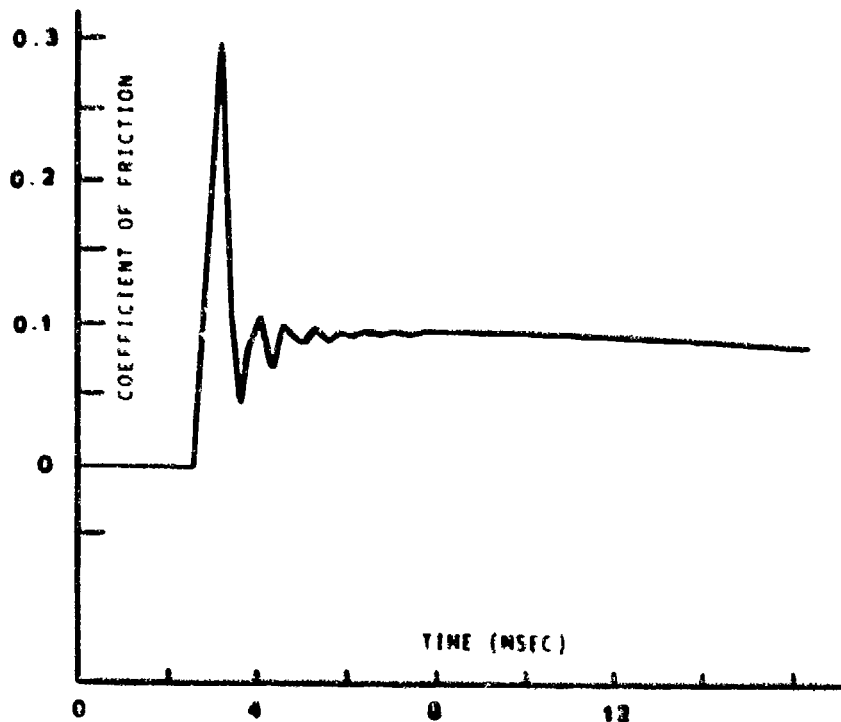


Figure 5. Coefficient of friction for no tightening

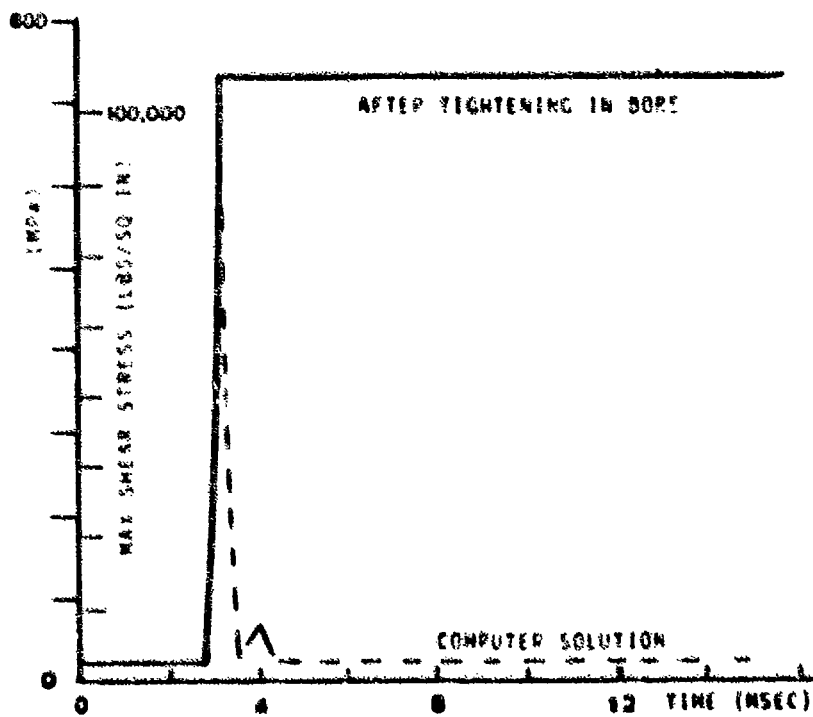


Figure 6. Shear stress at thread - coefficient of 0.1

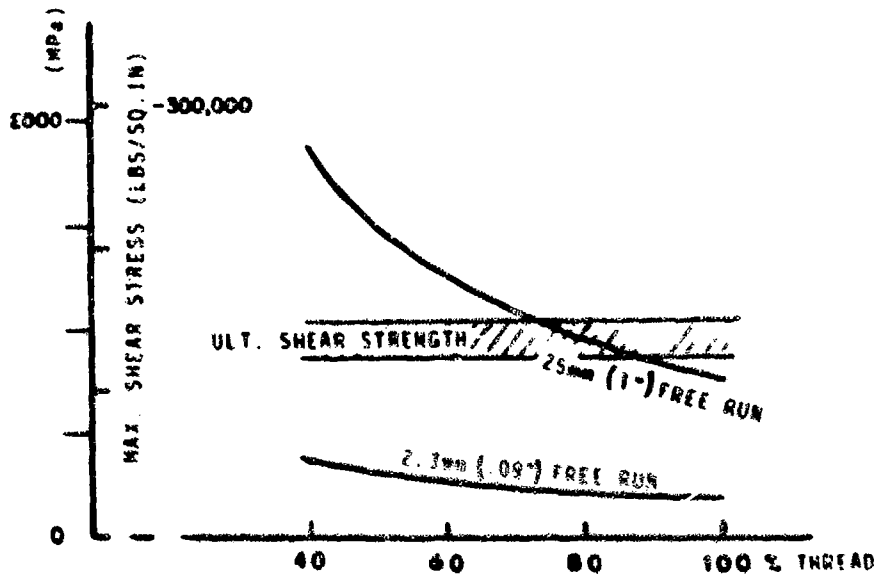


Figure 7. Maximum thread stress - coefficient of 0.1

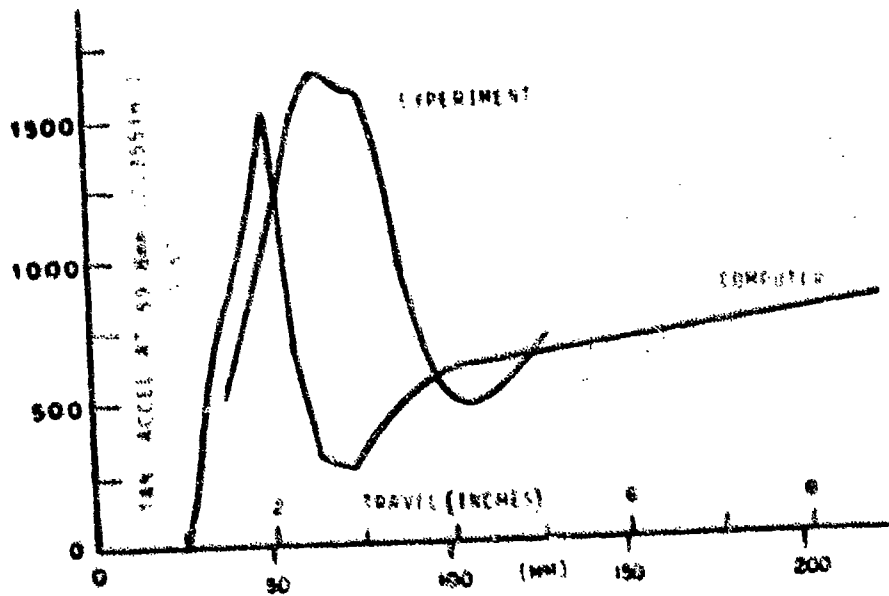
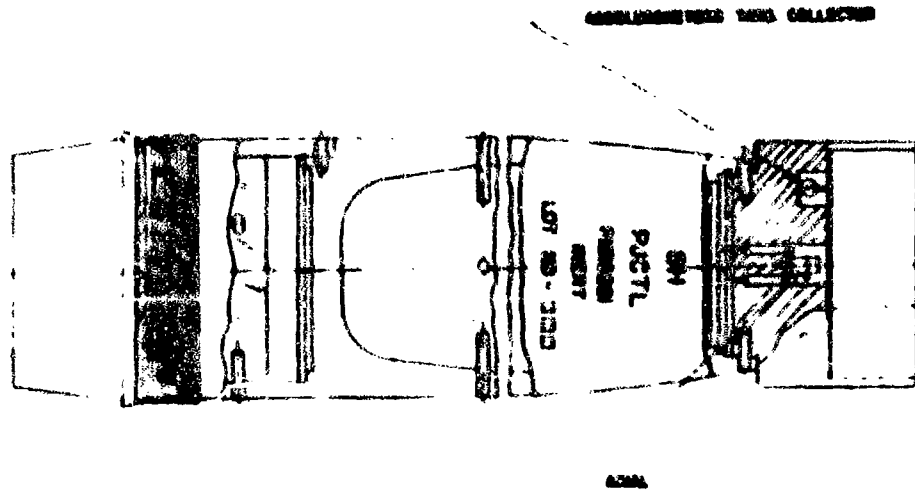


Figure 8. Experimental and computer results - 1 inch free run



TORSIONAL IMPULSE TEST ROUND

Figure 9. Torsional Impulse test round - 8-inch

8 INCH ROTATING BAND

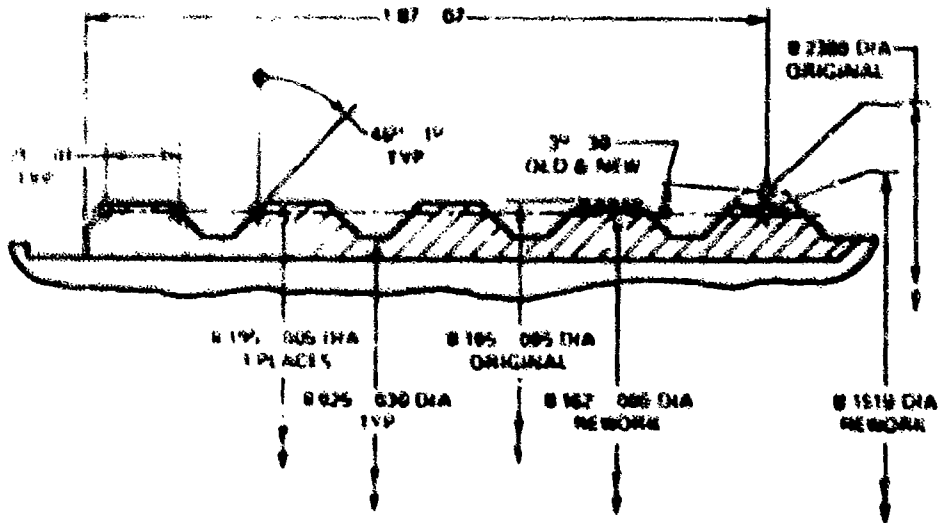


Figure 10. 8-inch rotating band - old and new

B-NCH ROTATING BAND STUDY - DR2442-MNR 77  
TANGENTIAL ACCELERATION VS DISTANCE - 5KG  
NEW TUBE, STD BAND

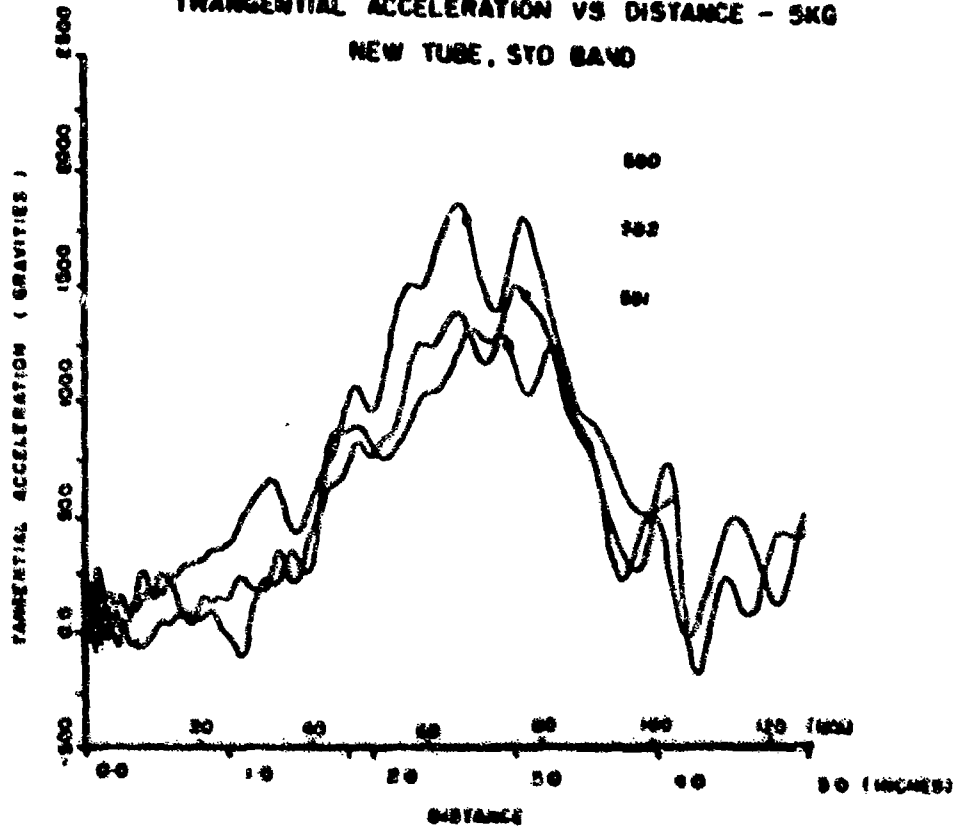


Figure 11. Tangential acceleration versus distance - old band

8-INCH ROTATING BAND STUDY - DR2442 - MRR 77  
TANGENTIAL ACCELERATION VS DISTANCE - 5KG  
NEW TUBE CUT BAND

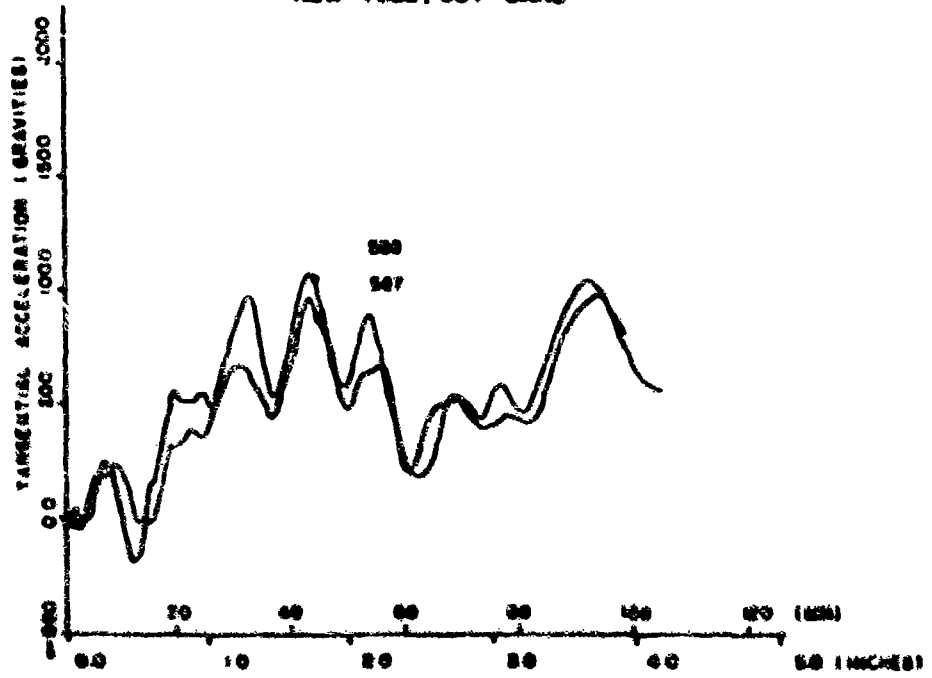


Figure 12. Tangential acceleration versus distance - new band

### AVERAGE TEST RESULTS

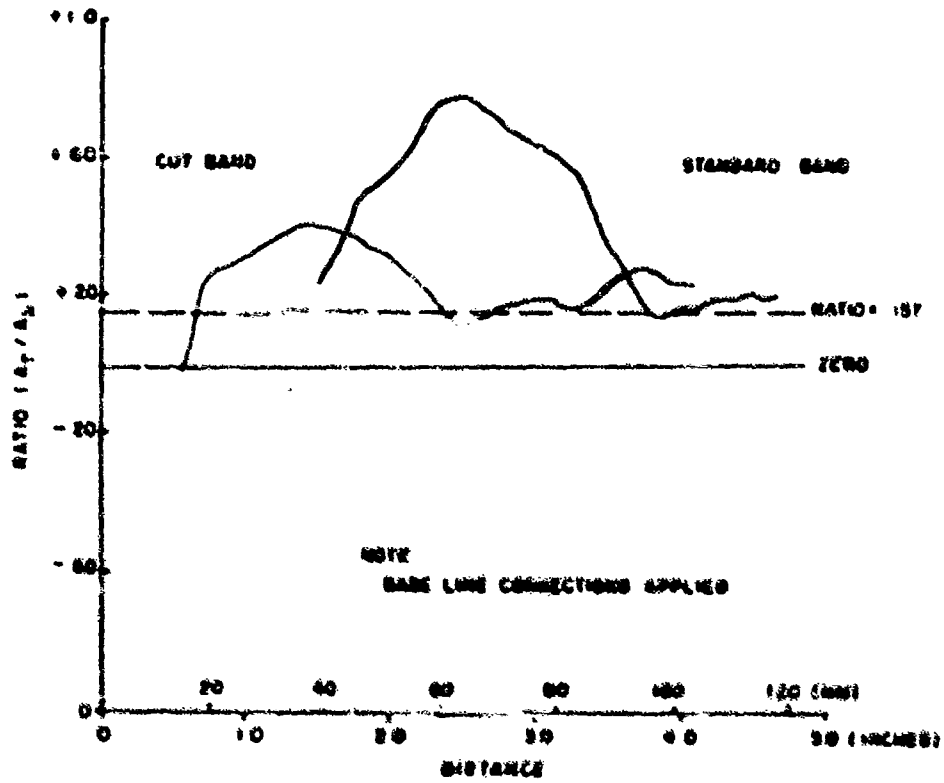
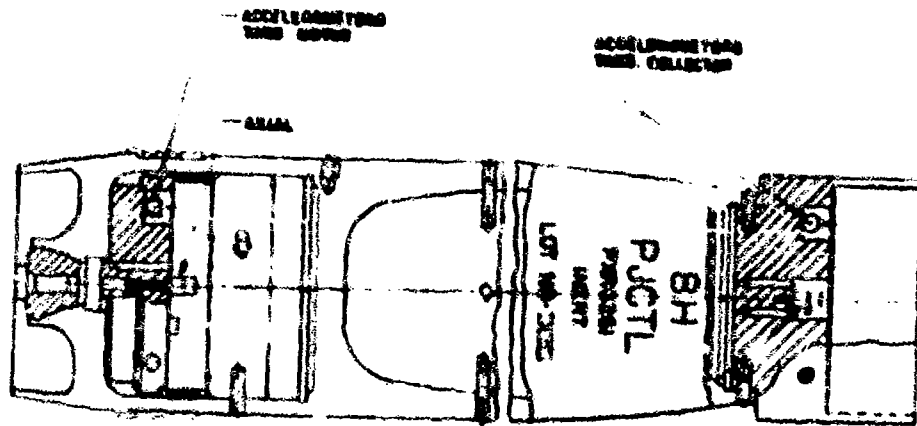


Figure 13. Averaged test results



TORSIONAL IMPULSE TEST ROUND

Figure 14. Torsional impulse test round - 8-inch

VIBRATION ACCELERATION TEST - 042503  
 RATIO - CELL CUP TANGENTIAL VIB. TO AXIAL ACCEL. (EX. JP)  
 R0130 076-ACCEL

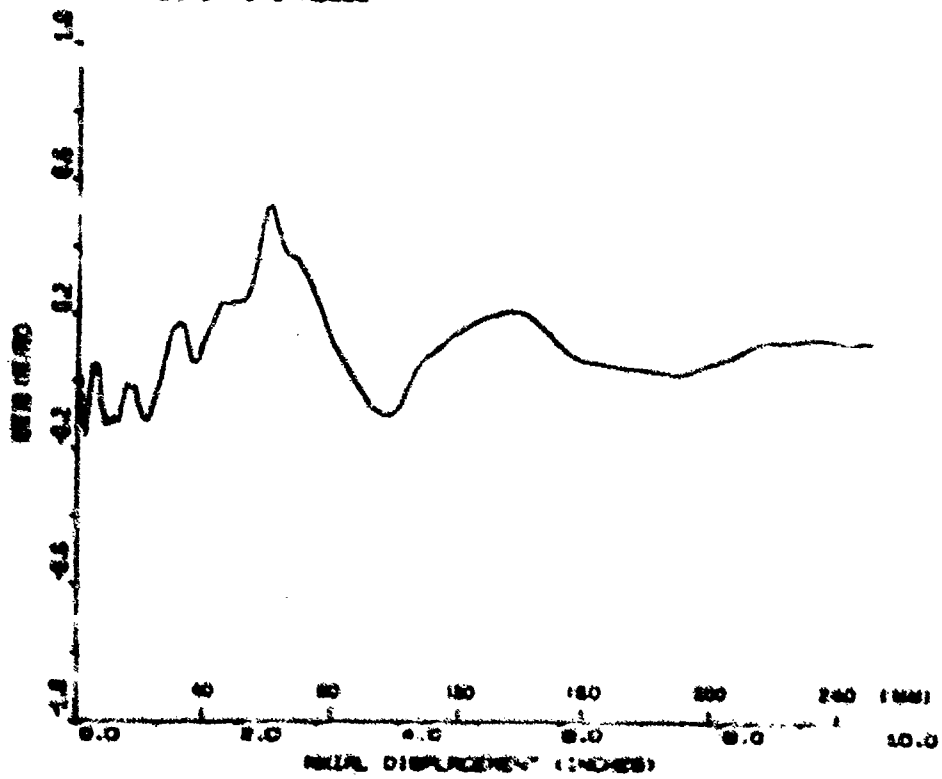


Figure 15. Ratio tangential to axial accelerations at collector cup - 8-inch

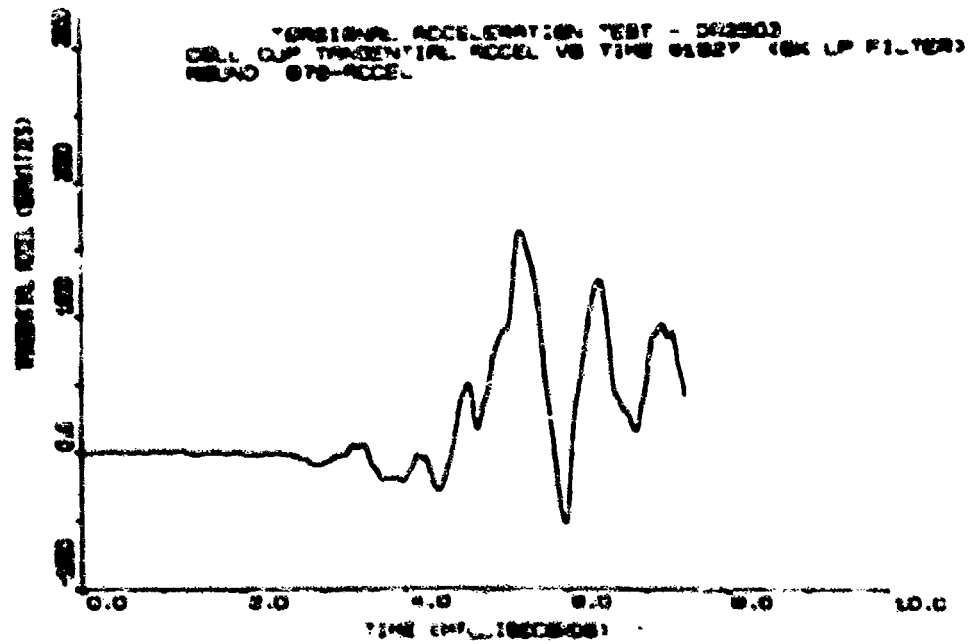


Figure 16. Tangential acceleration versus time - collector cup - 8-inch

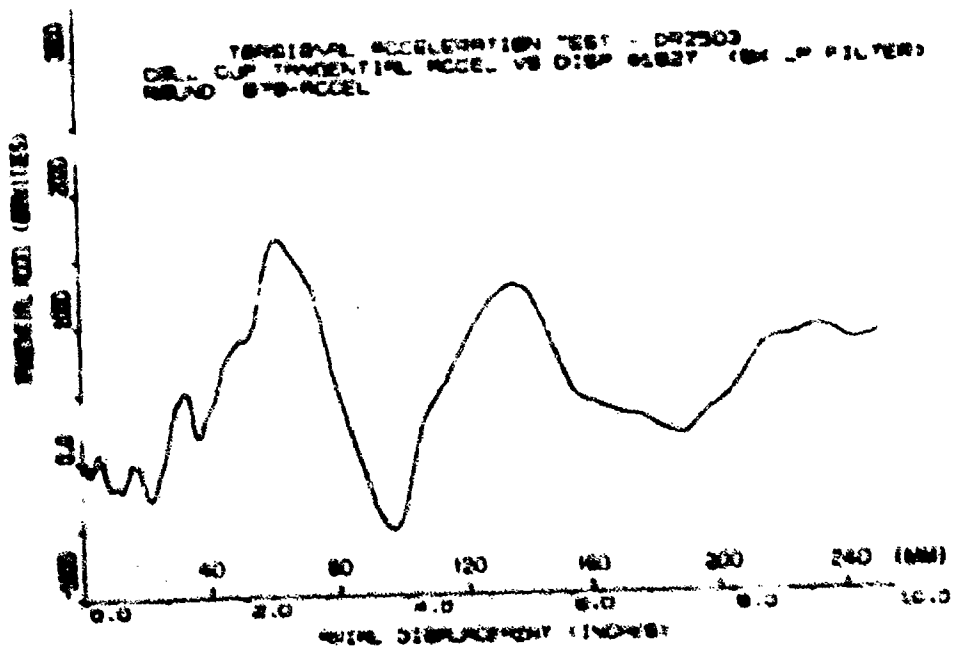


Figure 17. Tangential acceleration versus travel - collector cup - 8-inch

TENSIONAL ACCELERATION TEST - 042303  
COLLECTOR CLIP AXIAL ACCELERATION VS TIME FOR LP FILTERS  
RELOAD 078-RCEL

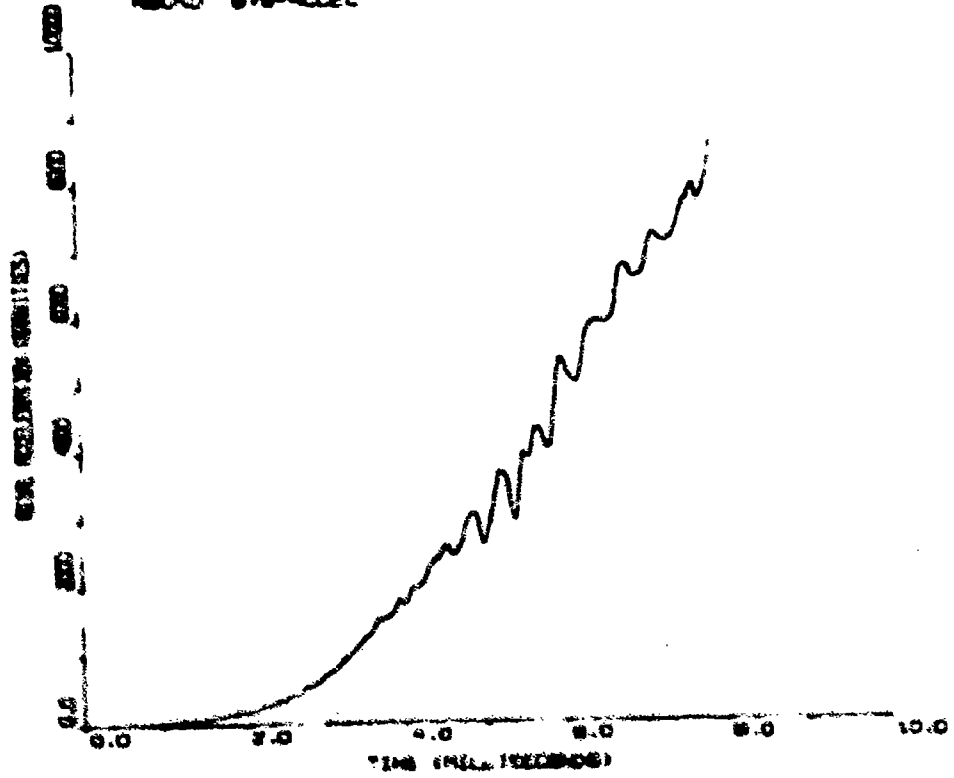


Figure 18. Axial acceleration versus time - 8-inch

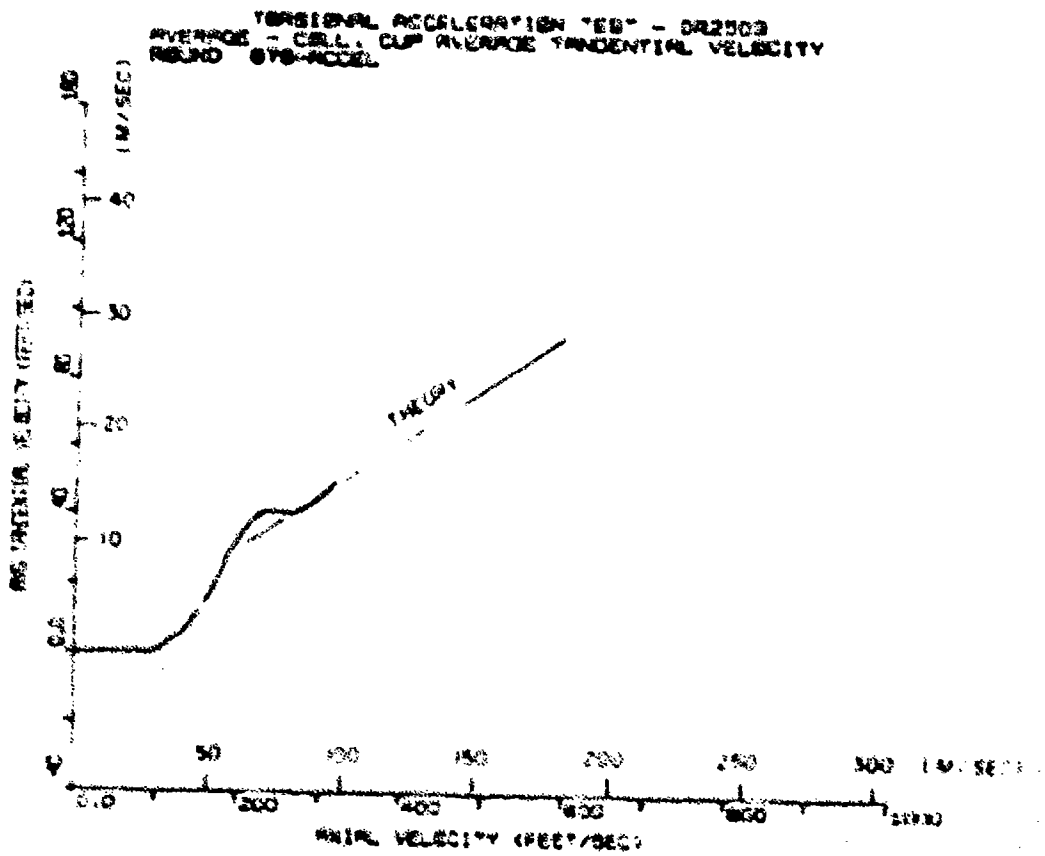
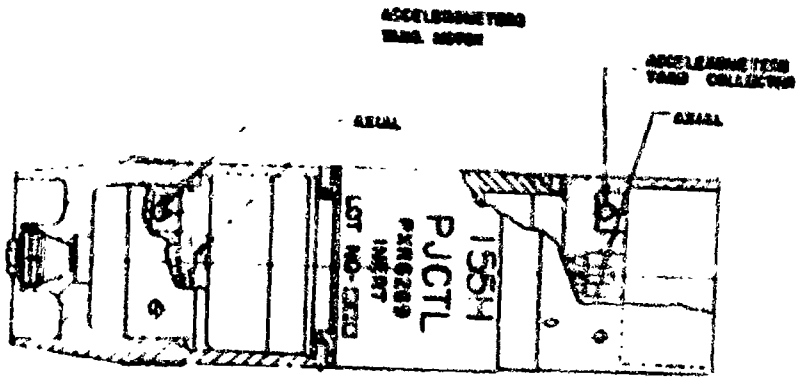


Figure 19. Tangential versus axial velocities - 8-inch



TORSIONAL IMPULSE TEST ROUND

Figure 20. Torsional impulse test round - 8-inch

107785 TANGENTIAL ACCELERATION TEST - 042503  
RATED - MOTOR BODY AND TANGENTIAL TO AXIAL ACCEL - FILTERED  
MODEL 2321-ACCEL

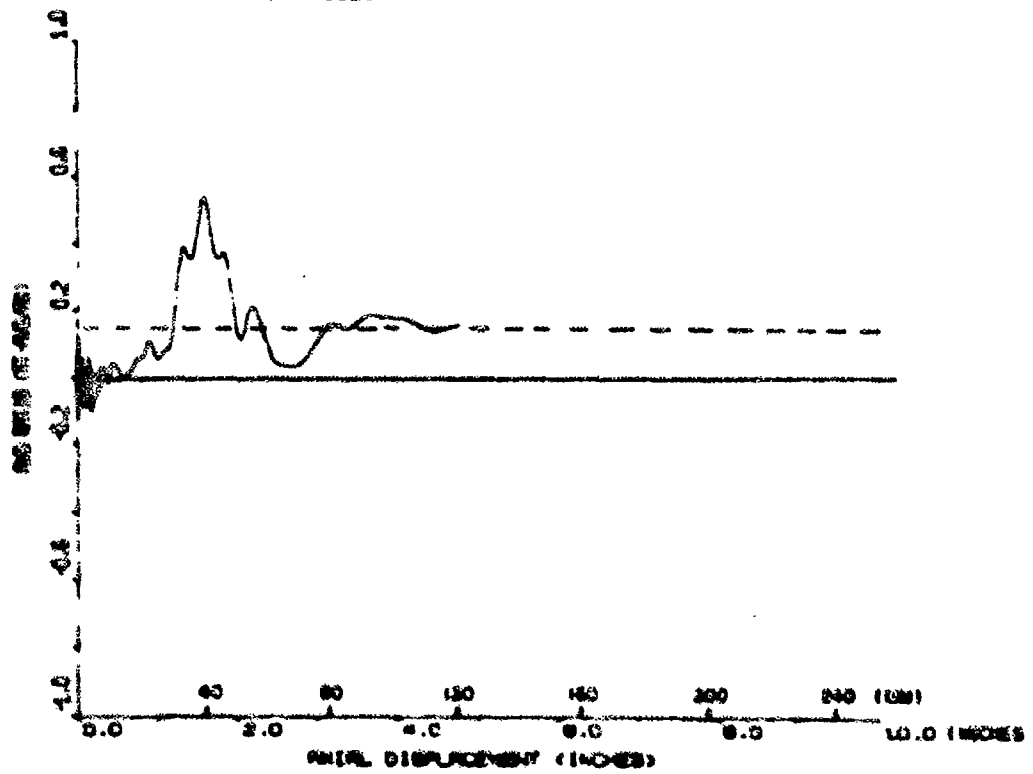


Figure 21. Ratio of tangential to axial accelerations versus travel at motor body - worn tube - 155-mm

UNITED TENSIONAL ACCELERATION TEST - 042803  
RATIO - MOTOR BODY AVG TANGENTIAL TO AXIAL ACCEL - FILTERED  
ROUND 2321-ACCEL

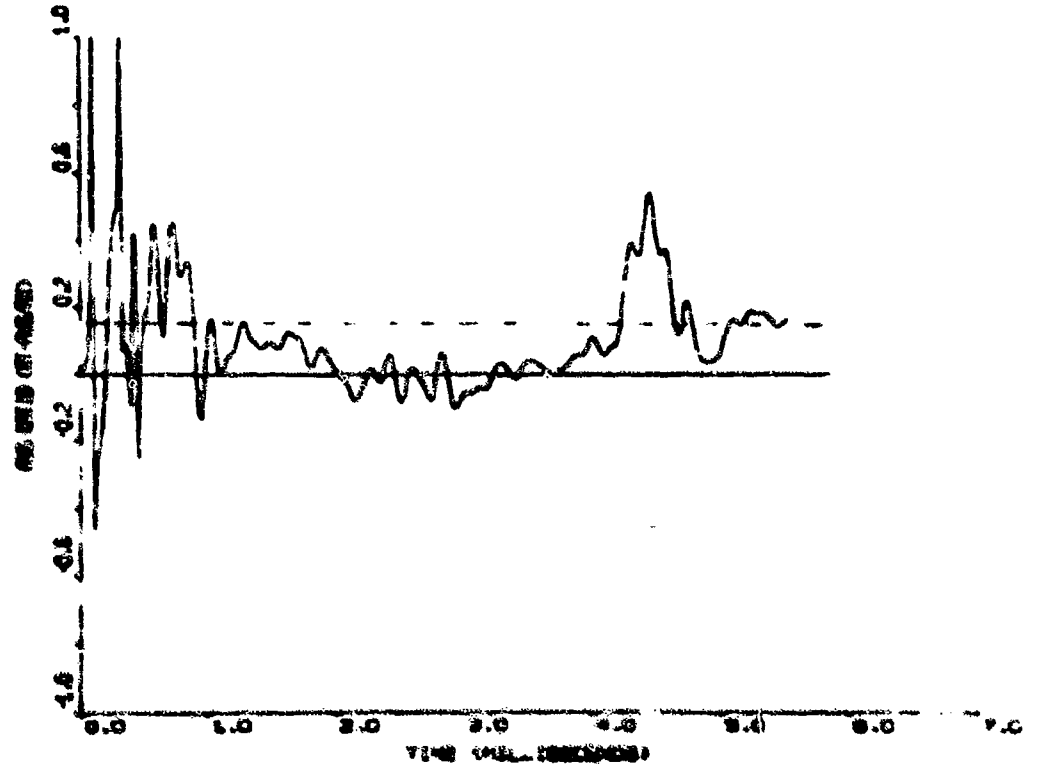


Figure 22. Ratio of tangential to axial accelerations versus time at motor body - worn tube - 155-mm

NOTES: TANGENTIAL ACCELERATION TEST - DAMPED  
MOTOR BODY TANGENTIAL ACCEL. RELAY VS TIME  
HOLDING 2221-ACCEL

F 80 110

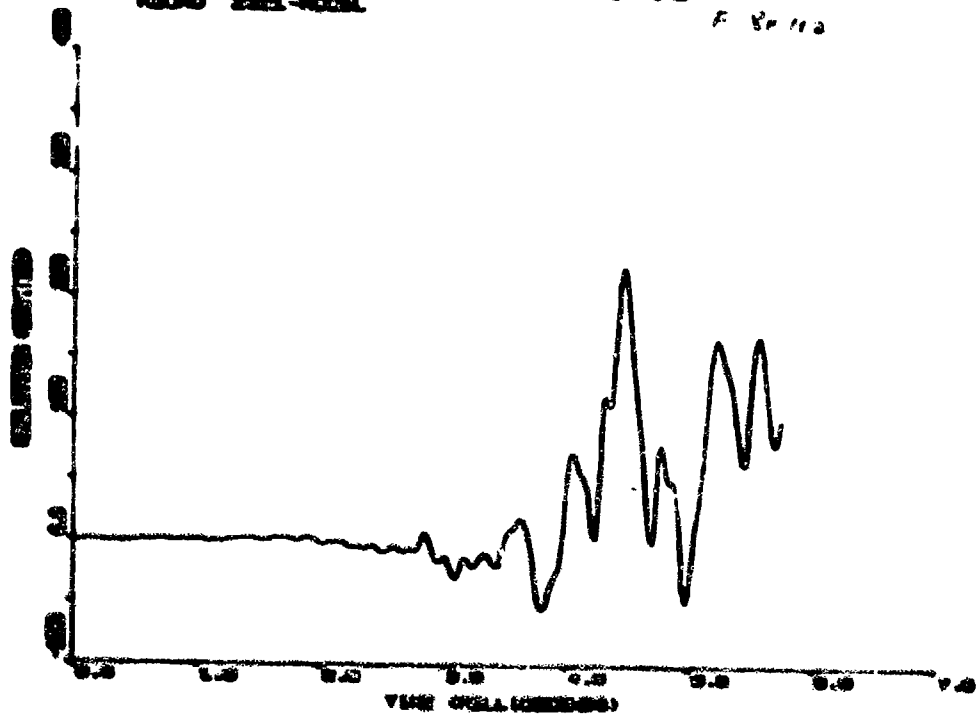


Figure 23. Tangential accelerometer #2127 at motor body versus time - 155-um

MOTOR TERMINAL ACCELERATION TEST - DAMPED  
MOTOR BODY TANGENTIAL ACCEL. SIGNAL VS TIME F 50 Hz  
SIGNAL 2500-0000

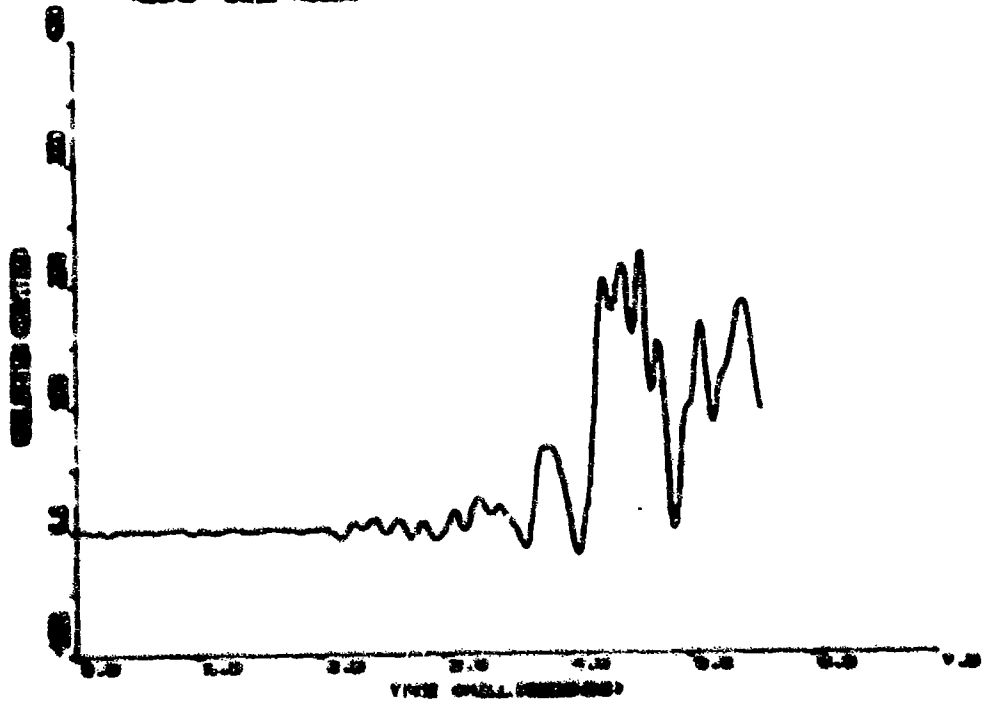


Figure 24. Tangential accelerometer #2130 at motor body versus time - 155-um

AXIAL ACCELERATION VERSUS TIME - 155-AM  
 155-AM  
 155-AM

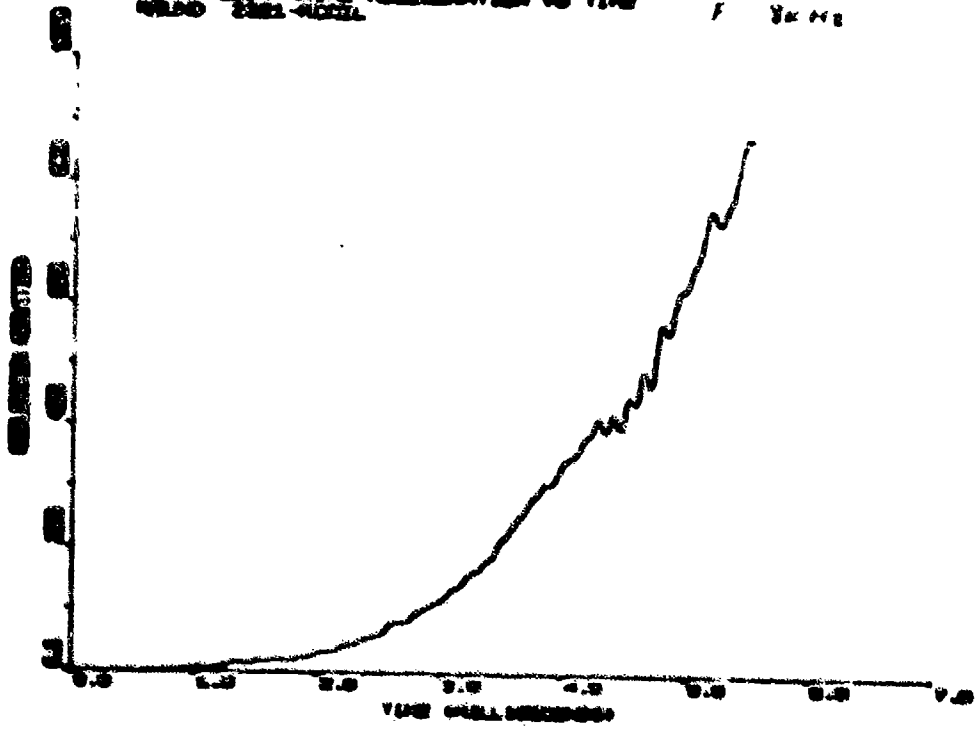


Figure 25. Axial accelerometer versus time - 155-AM

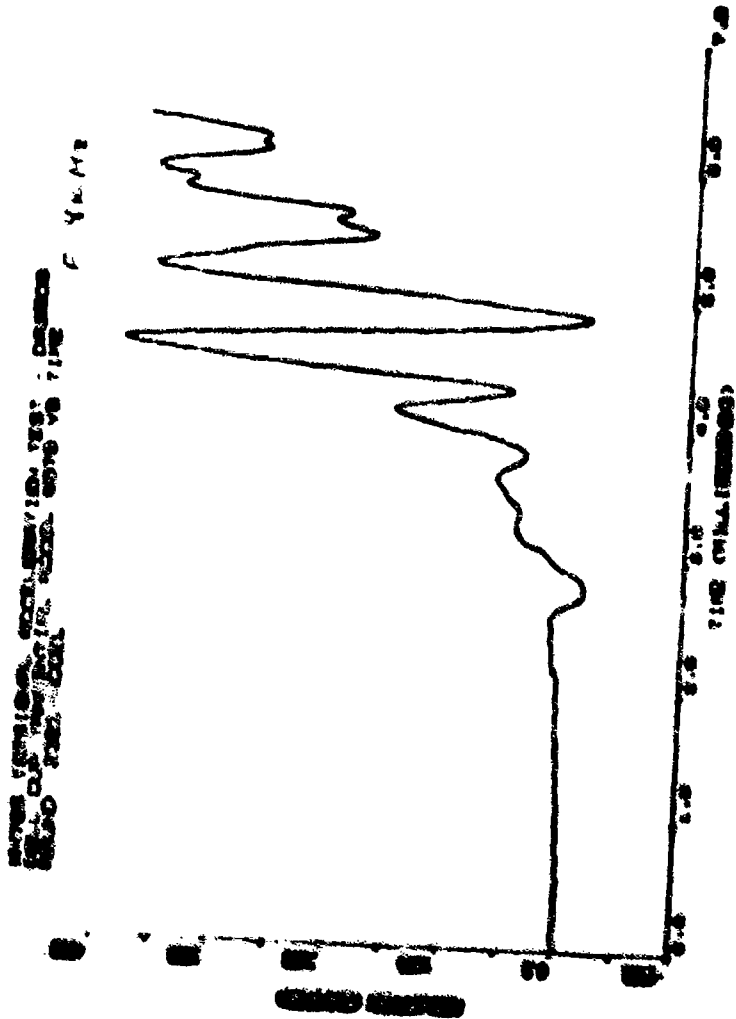


Figure 26. Tangential accelerometer 0979 at collector cup versus time - 155-000

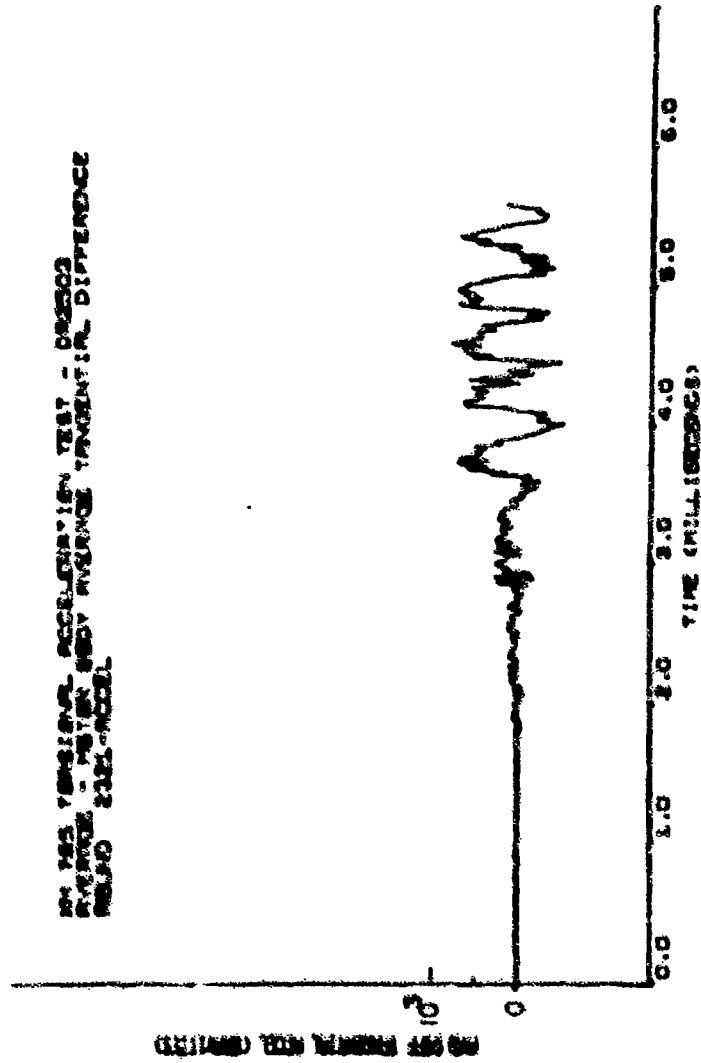


Figure 27. Difference in tangential accelerometers versus time round #2321 in  
 worn tube - 135-000

IN THE TANGENTIAL ACCELERATION TEST - D88003  
 RECORDS - WITH BODY AVERAGE TANGENTIAL DIFFERENCE  
 BEING 2.80-MILL

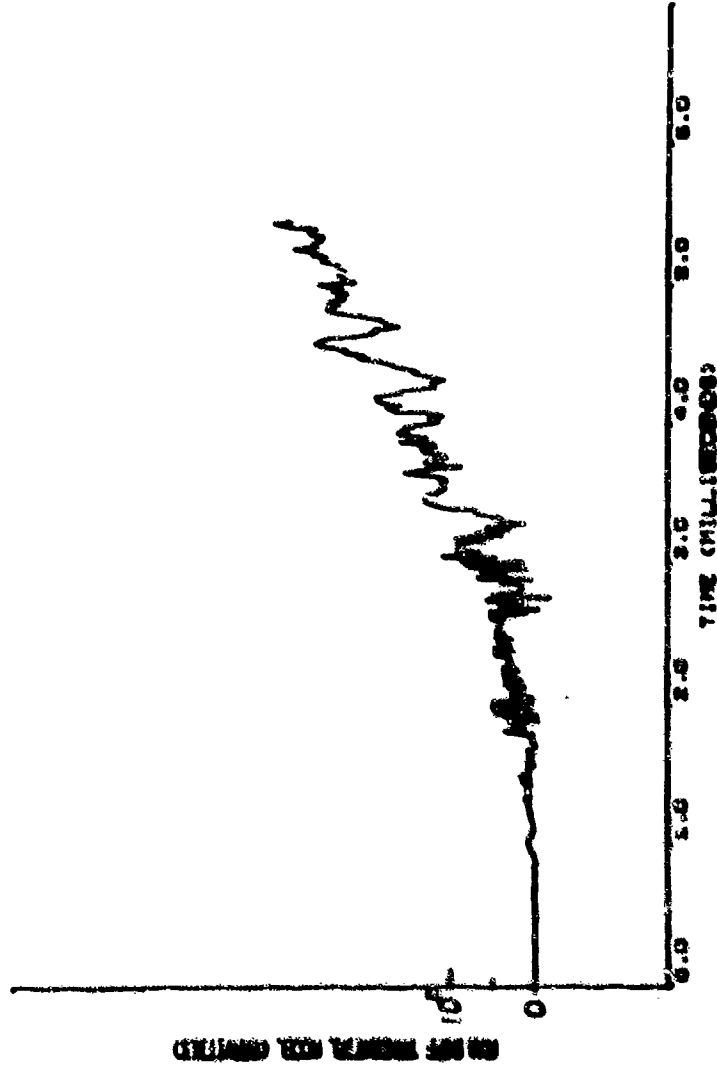


Figure 28. Difference in tangential accelerometers versus time round #2320 in  
 worm tube - 155-44

FOR THE TANGENTIAL VELOCITY DISTRIBUTION TEST - DRUMS  
 RUCORZ - PULVERIZER - PULVERIZER TANGENTIAL VELOCITY  
 RUCORZ - PULVERIZER

511 078

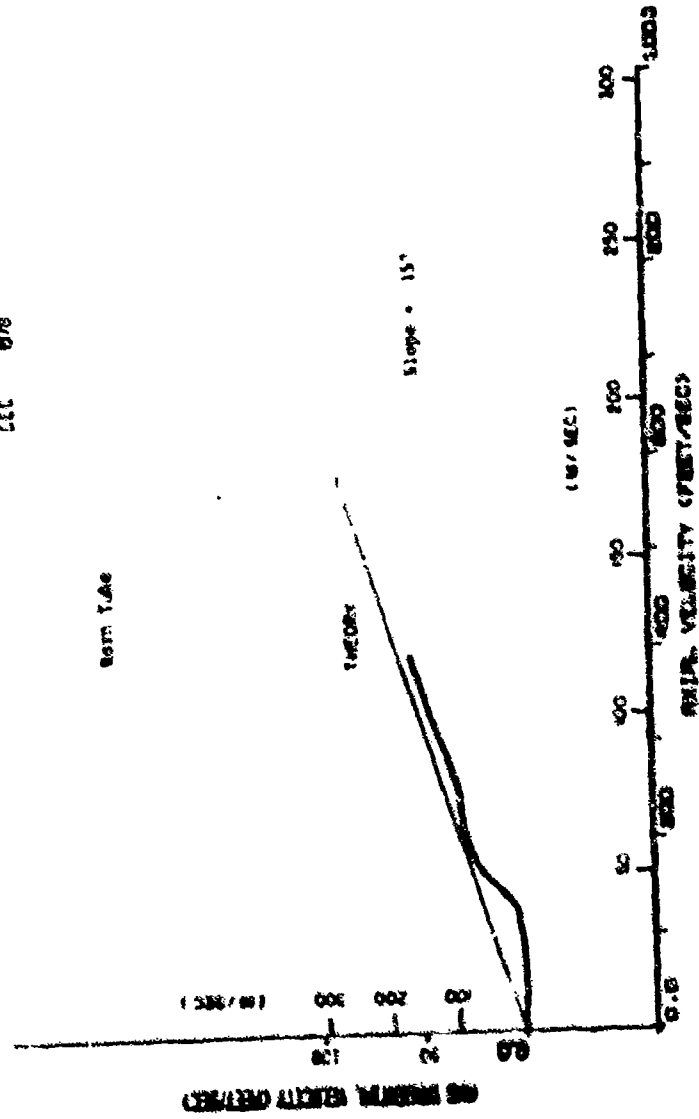


Figure 29. Tangential versus axial velocities - 155-mm

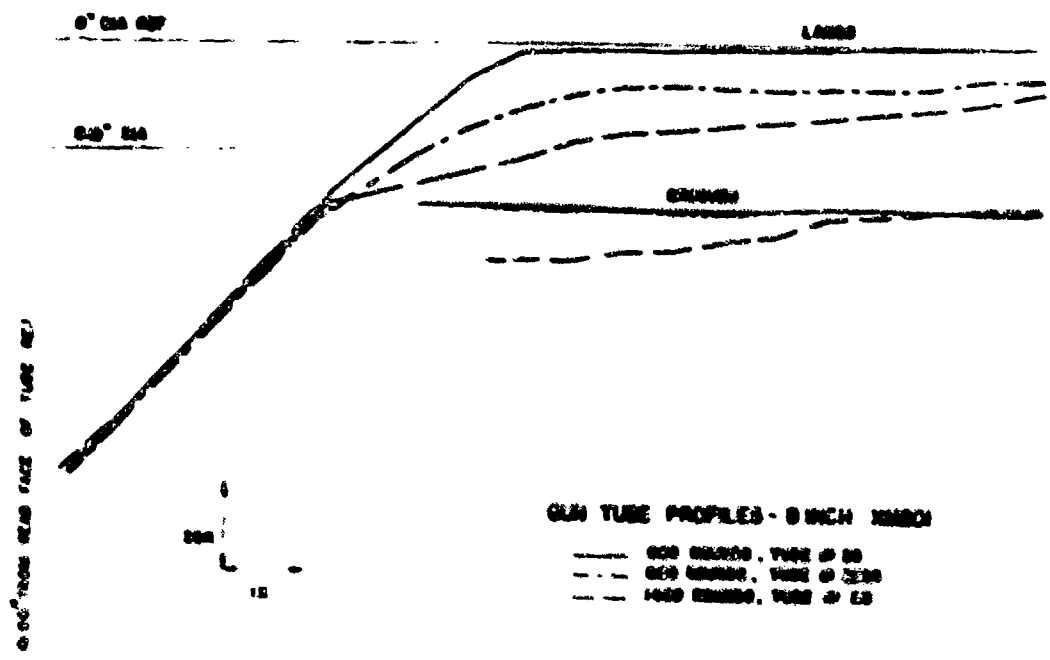


Figure 30. Gun tube profiles - 8 inch XM201

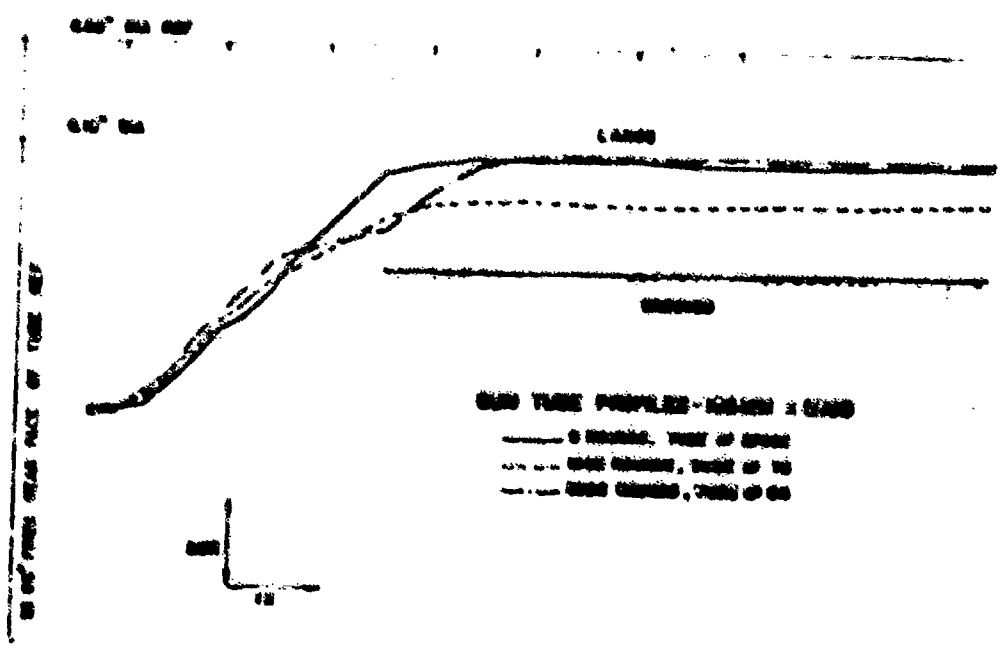


Figure 31. Gun tube profiles - 155 mm XM199

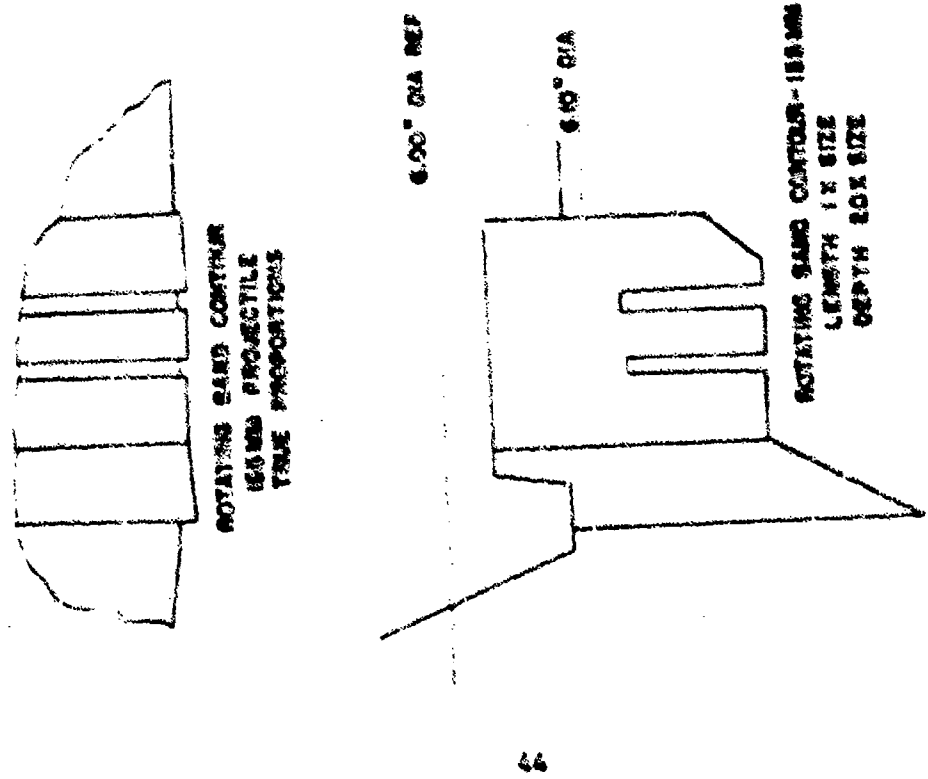
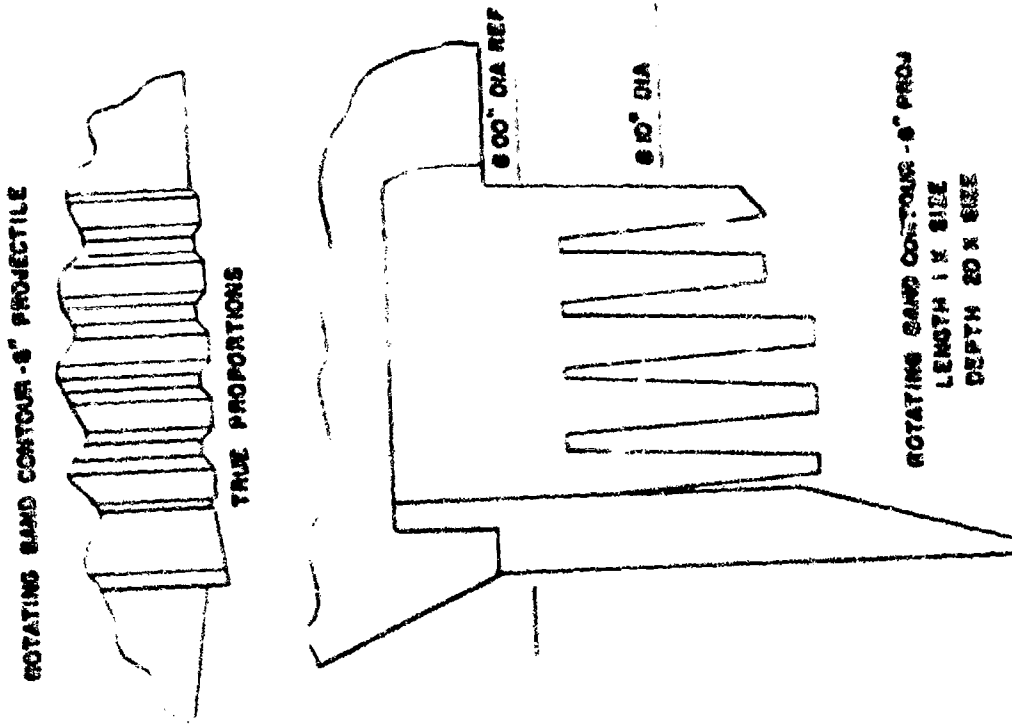
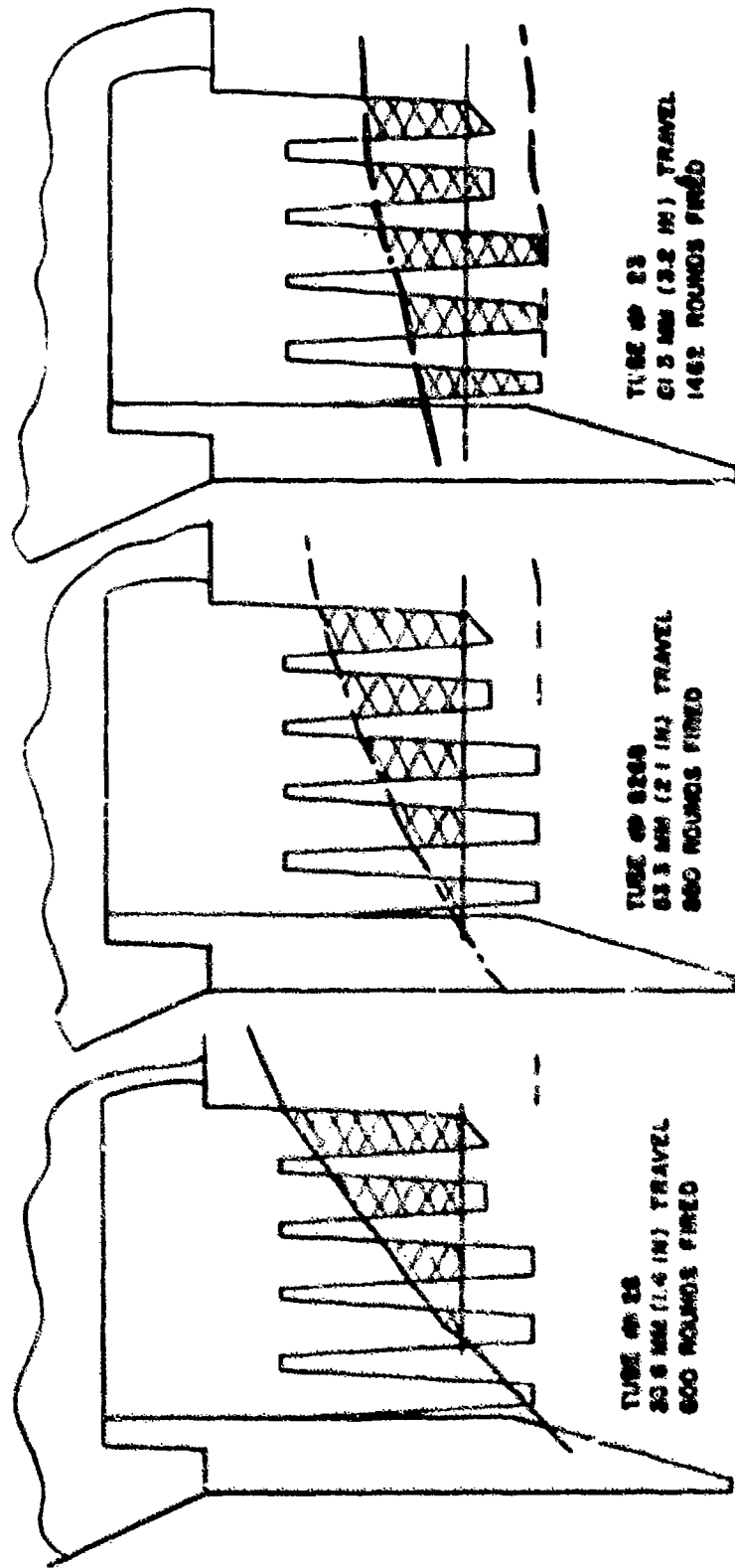
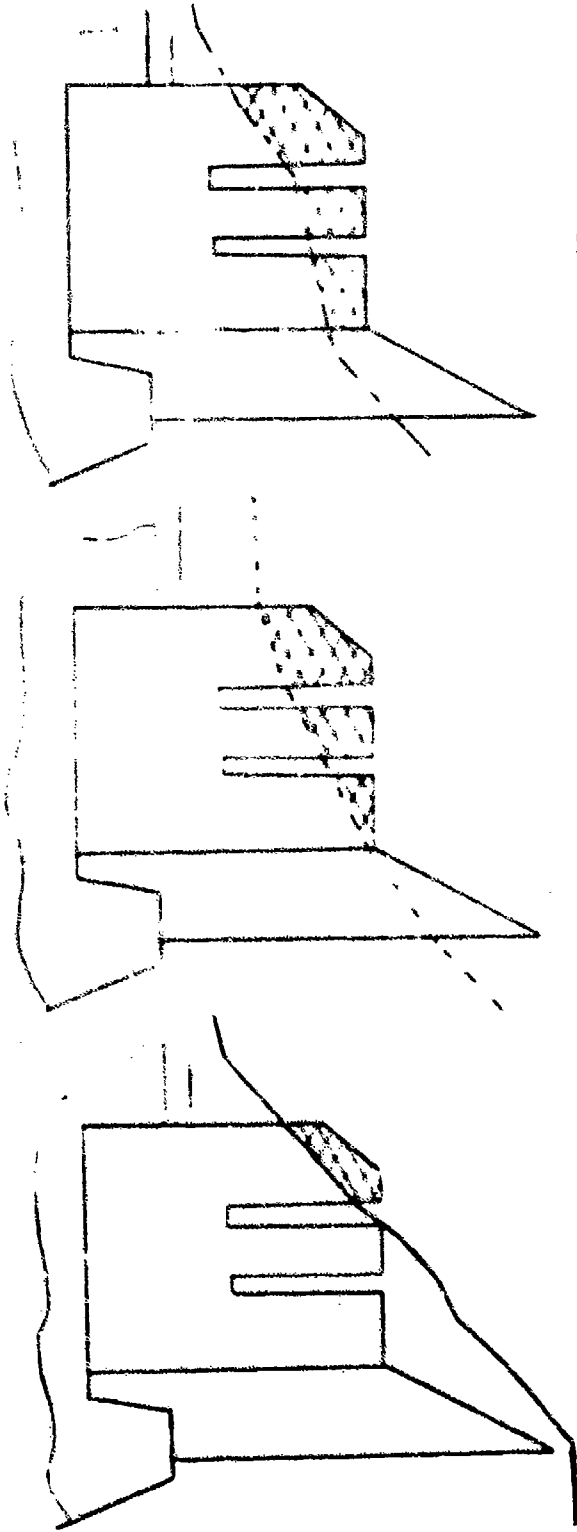


Figure 32. Silhouettes of rotating bands - 155-mm and 9-inch projectiles



**BAND / RIFLING OVERLAP AT TORSIONAL PULSE 8 INCH**

Figure 13. Overlap of band in rifling profiles - 8-inch



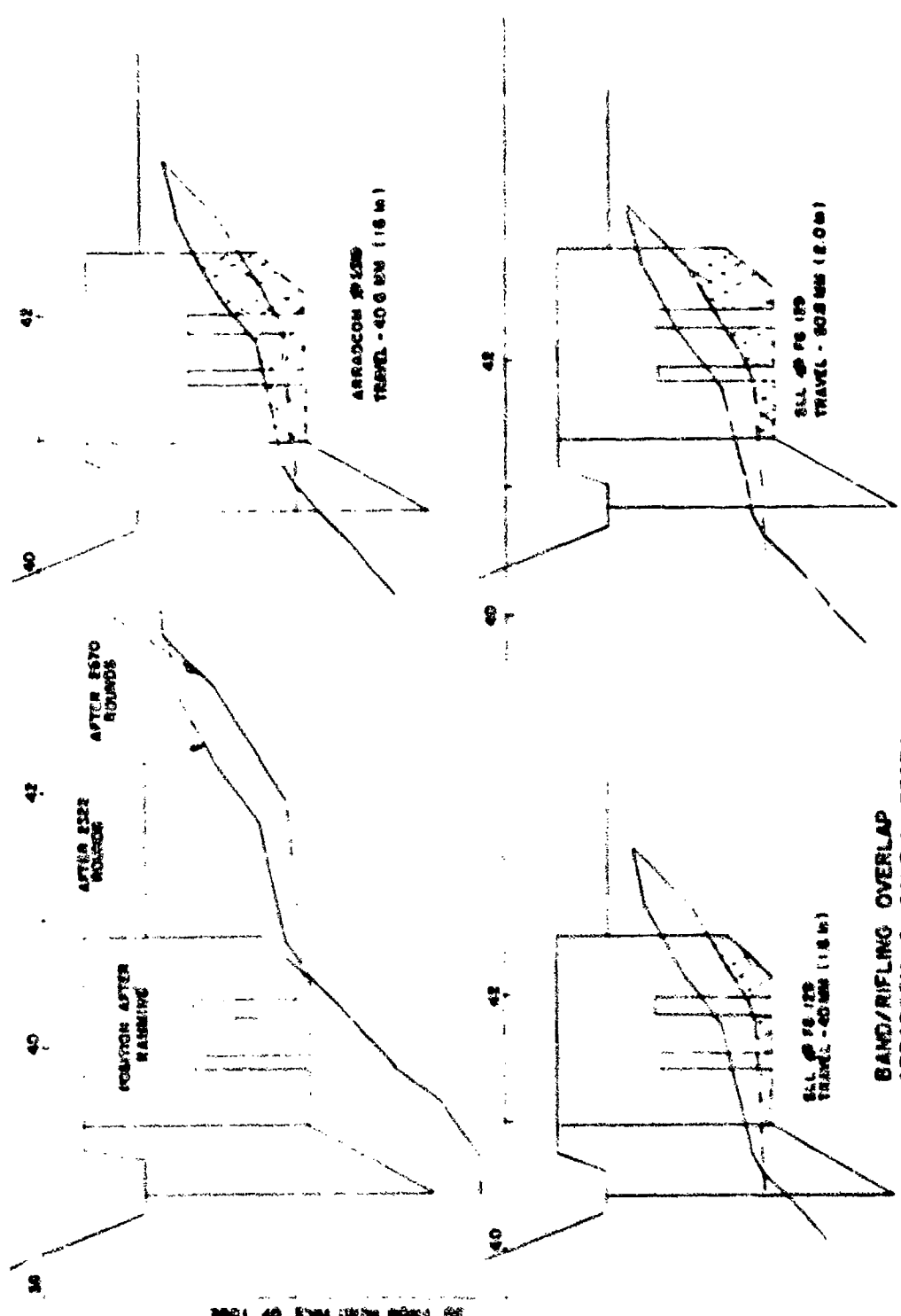
TUBE # 27882  
 78 MM (3 IN) TRAVEL  
 6 ROUNDS FIRED

TUBE # 75  
 20.5 MM (1.2 IN) TRAVEL  
 1065 ROUNDS FIRED

TUBE # 63  
 28.0 MM (1.6 IN) TRAVEL  
 2322 ROUNDS FIRED

**BAND / RIFLING OVERLAP AT TORSIONAL  
 PULSE 156 MM PROJECTILE**

Figure 14. Overlap of band in rifling profiles - 155-mm



**BAND/RIFLING OVERLAP  
ARRADCOM & SANDIA TESTS**

Figure 35. Band/rifling overlap in ARRADCOM and Sandia tests

DISTRIBUTION LIST

Administrator  
Defense Technical Information Center(12)  
ATTN: Accessions Division  
Cameron Station  
Alexandria, VA 22314

Director  
U.S. Army Materiel Systems Analysis Activity  
ATTN: DRXSY-MP  
Aberdeen Proving Ground, MD 21005

Commander  
U.S. Army Armament Research and  
Development Command  
Weapons Systems Concepts Team  
ATTN: DRDAR-ACW  
APG, Edgewood Area, MD 21010

Commander/Director  
Chemical Systems Laboratory  
U.S. Army Armament Research and  
Development Command  
ATTN: DRDAR-CLJ-L  
APG, Edgewood Area, MD 21010

Director  
Ballistics Research Laboratory  
U.S. Army Armament Research and  
Development Command  
ATTN: DRDAR-TSB-S  
Aberdeen Proving Ground, MD 21005

Chief  
Benet Weapons Laboratory, LCWSL  
U.S. Army Armament Research and  
Development Command  
ATTN: DRDAR-LCB-TL  
Watervliet, NY 12189

Commander  
U.S. Army Armament Materiel  
Readiness Command  
ATTN: DRSAR-LEP-L  
Rock Island, IL 61299

Director  
U.S. Army TRADOC System  
Analysis Activity  
ATTN: ATAA-SL (Technical Library)  
White Sands Missile Range, NM 88002

Director  
Defense Research and Engineering  
ATTN: Technical Library  
Washington, DC 20301

Director  
Lawrence Livermore Laboratory  
ATTN: G.L. Goudreau  
Roger Werne  
P.O. Box 808  
Livermore, CA 94550

Director  
Los Alamos Scientific Laboratory  
ATTN: R. L. Peeters  
Richard Browning  
P.O. Box 1663  
Los Alamos, NM 87544

Sandia Laboratories  
ATTN: G. A. Benedetti, B122  
M. L. Callabresi, B122  
P.O. Box 969  
Livermore, CA 94550

Director of Army Research  
Dept of the Army  
ATTN: DAMA-ARZ-A  
Washington, DC 20310

Asst. Dir. for Laboratory Activities  
Dept of the Army  
ATTN: DAMA-ARZ-C  
Washington, DC 20310

Asst. Dir. for Research Programs  
Dept. of the Army  
ATTN: DAMA-ARZ-D  
Washington, DC 20310

Director  
U.S. Army TRADOC System  
Analysis Activity  
ATTN: ATAA-SL (Technical Library)  
White Sands Missile Range, NM 88002

Director  
Defense Research and Engineering  
ATTN: Technical Library  
Washington, DC 20301

Director  
Lawrence Livermore Laboratory  
ATTN: G.L. Goudreau  
Roger Werne  
P.O. Box 808  
Livermore, CA 94550

Director  
Los Alamos Scientific Laboratory  
ATTN: R. L. Peeters  
Richard Browning  
P.O. Box 1663  
Los Alamos, NM 87544

Sandia Laboratories  
ATTN: G. A. Benedetti, B122  
M. L. Callabresi, B122  
P.O. Box 969  
Livermore, CA 94550

Director of Army Research  
Dept of the Army  
ATTN: DAMA-ARZ-A  
Washington, DC 20310

Asst. Dir. for Laboratory Activities  
Dept of the Army  
ATTN: DAMA-ARZ-C  
Washington, DC 20310

Asst. Dir. for Research Programs  
Dept. of the Army  
ATTN: DAMA-ARZ-D  
Washington, DC 20310

Deputy Comander for Materiel Development  
Dept of the Army  
ATTN: DRCMDM-ST  
Alexandria, VA 22333

Associate Director for Systems Development  
ATTN: DRCDE-D  
Alexandria, VA 22333

Project Manager  
Cannon Artillery Weapon System  
ATTN: DRCPM-CAWS, Mr. Menke  
Dover, NJ 07801

Director Armament Systems Directorate  
ATTN: DRDAR-AS  
Dover, NJ 07801

Project Manager  
Nuclear Munitions  
ATTN: DRCPM-NUC  
Dover, NJ 07801

Commander  
U.S. Army Armament Research & Development Command  
ATTN: DRDAR-TD, R. Weigle  
DRDAR-BLP, L. A. Watermeier  
S. S. Lentz  
I. W. May  
B. P. Burns  
DRDAR-BLT, J. M. Santiago  
DRDAR-LC, J. Frazier  
DRDAR-LCA, W. Benson  
H. Fair  
L. Rosendorf  
DRDAR-LCB, R. Montgomery  
T. Simkins  
DRDAR-LCE, D. A. Wiegand  
W. E. Voreck  
DRDAR-LCM, Mr. S. Kaplowitz  
DRDAR-LCN, F. Saxe  
G. Demitrack  
J. Drake  
C. J. Spinelli  
S. DiDomenico  
A. Franz  
H. Smith

DRDAR-LCN, F. Scerbo  
A. E. Schmidlin  
DRDAR-LCS, J. Gregorits  
R. Corn  
DRDAR-LCU, A. Moss  
G. Jackman  
R. Botticelli  
S. Harnett  
V. Ilardi  
DRDAR-LCW, H. Garver  
DRDAR-MS, D. Grobstein  
DRDAR-NC, C. E. Fields  
DRDAR-SC, D. Gyorog  
S. Jacobson  
DRDAR-SE, M.D. Brailsford  
DRDAR-TSS (5)

Dover, NJ 07801